

國立交通大學

電子物理研究所

碩士論文

電閘極對二維拓樸材料(HgTe/CdTe)之邊緣  
態和量子傳輸的影響

EFFECTS OF ELECTRIC-GATING ON THE  
EDGE-STATES AND QUANTUM TRANSPORT IN 2D  
TOPOLOGICAL MATERIALS (HgTe)

研究生：陳文長  
指導教授：朱仲夏 博士

中華民國一百零一年 2 月

# 二維拓樸材料(HgTe/CdTe)中電閘極對邊緣態與量子傳輸的影響

學生：陳文長

指導教授：朱仲夏教授

電子物理系

國立交通大學

## 摘要

此論文包含三部分：HgTe/CdTe 量子井的拓樸特徵、有或無分裂閘極之柱狀量子自旋霍爾井的電子能譜以及在柱狀 HgTe/CdTe 量子自旋霍爾井中經過由有限長的分裂閘極所構成之量子接點的量子傳輸。

於第一部分，吾做出及展示出 HgTe/CdTe 系統的  $Z_2$  拓樸不變性。於第二部分，吾證明若邊於態存在則其維持於柱狀量子自旋霍爾井的邊界而非由分裂閘極所定義出的邊界。最後，第三部分，在量子接點組態下，電導中有著值得關注的結構被發現。此結構與邊緣態的關係將會被探討。

---

EFFECTS OF ELECTRIC-GATING ON THE EDGE-STATES AND  
QUANTUM TRANSPORT IN 2D TOPOLOGICAL MATERIALS  
(HgTe/CdTe).

Student: Tran Van Truong

Supervisor: Prof. Chon-Saar Chu

Department of Electrophysics  
National Chiao-Tung University

### Abstract

This work covers three parts: the topological features of the HgTe/CdTe quantum well, the electronic spectrum of quantum spin Hall bar with or without a split-gated configuration, and the quantum transport through a quantum point contact formed by a finite-length split-gate on a HgTe/CdTe quantum spin Hall bar.

In the first part, we work out and demonstrate the  $Z_2$  topological invariant of HgTe/CdTe system. In the second part, we show that the edge states, when exist, will remain locating to the vicinity of the boundaries of the quantum spin Hall bar rather than to the boundaries defined by the split gates. Finally, in the third part, interesting structures in the conductance are found. Relation of these structures to the edge states will be explored.

---

### **Acknowledgment.**

To have these results, I got a lot of support from my supervisor and friends. So, I would like to send my deepest gratitude to my professor. Thank professor very much for your upbringing and advice in the past days.

I am also grateful to my friends very much. Thank you, Luyao, Chiu, Rong Shing, Tlay, Wen Li, Cosin, SuHao and other ones for helping me in studying as well as in living. I believe that without your help, my work would not have been possible.

Finally, I would like to say that I love every one here, I love NCTU and I love Taiwan very much. Taiwanese people are very friendly and lovely. I will never forget you.

Thank all.



# Contents

<b>Abstract in English</b>	<b>ii</b>
<b>Acknowledgment</b>	<b>iii</b>
<b>List of figures</b>	<b>vi</b>
<b>1 Introduction</b>	<b>1</b>
1.1 Background . . . . .	1
1.1.1 Topological insulator(TI). . . . .	1
1.1.2 Time reversal symmetry . . . . .	3
1.1.3 Spin-orbit interaction. . . . .	4
1.1.4 Hall effects. . . . .	5
1.2 Motivation. . . . .	7
1.3 A guiding tour to the thesis. . . . .	11
<b>2 Study topological features of HgTe/CdTe material via Berry curvature and Chern number.</b>	<b>12</b>
2.1 Berry phase and Berry curvature. . . . .	13
2.1.1 Overview of Berry phase and Berry curvature. . . . .	13
2.1.2 The Berry curvature in HgTe/CdTe topological insulators. . . . .	15
2.2 Chern number. . . . .	21
2.3 The analysis of the result of Berry curvature and Chern number. . . . .	22
2.3.1 The Berry curvature under the time reversal symmetry. . . . .	22

2.3.2	$Z_2$ invariant. . . . .	23
2.4	Brief summary. . . . .	24
<b>3</b>	<b>Electronic spectrum of a HgTe/CdTe quantum Hall bar.</b>	<b>25</b>
3.1	First approach: using sine functions as basic. . . . .	25
3.2	Second approach: using exponent functions as trial functions. . . . .	31
3.3	Comparing results of two approaches. . . . .	36
3.4	Brief summary. . . . .	37
<b>4</b>	<b>Electronic band of a split gated HgTe/CdTe quantum Hall bar</b>	<b>38</b>
4.1	The equation to determine energy dispersion of the new system. . . . .	38
4.2	Result of energy dispersion. . . . .	40
4.2.1	Special cases: $d = 0$ and $d = W/2$ . . . . .	41
4.2.2	Result for other cases. . . . .	41
4.3	Edge states in the system. . . . .	42
4.4	Brief summary. . . . .	45
<b>5</b>	<b>Quantum transport in HgTe/CdTe quantum point contact.</b>	<b>47</b>
5.1	The equation to determine $k_x$ and $\chi_n$ . . . . .	48
5.2	The wave function in each region and the equation to determine the coefficients $r_m, t_m$ . . . . .	51
5.3	Results of conductance and discussion. . . . .	55
<b>6</b>	<b>Conclusion and proposal for future work.</b>	<b>59</b>
6.1	Conclusion . . . . .	59
6.2	Future work. . . . .	60
<b>A</b>	<b>Appendix</b>	<b>61</b>

# List of Figures

1.1	Electric band. . . . .	2
1.2	HgTe/CdTe quantum well at thickness greater then and less then the critical thickness. . . . .	8
1.3	The two split gates system: HgTe/CdTe bar with electric potentials are applied at transerve boundaries. . . . .	10
1.4	Quantum transport model is proposed from the system of HgTe/CdTe bar with electric potentials are applied at transerve boundaries (QPC system). . . . .	10
2.1	The plotting of the Berry curvature for analytical result. . . . .	20
2.2	Edge states in quantum spin Hall insulator at the interface between a Quantum spin Hall insulator and an ordinary insulator. . . . .	24
3.1	The HgTe/CdTe bar system. . . . .	26
3.2	Energy dispersion of HgTe/CdTe bar system. Potential is $V=0$ meV. The width of system is $W=100$ nm for (a) and $W=200$ nm for (b). . . . .	28
3.3	Energy dispersion of HgTe/CdTe bar system. The width of system is $W=100$ nm. Potential is $V=0$ meV for (a) and $V=10$ meV for (b). . . . .	29
3.4	(a) Density of edge states at $k=0.05$ and $k=-0.05$ nm. Other parameters are $W=200$ nm, $V=0$ meV. (b) Edge states at each boundary. . . . .	29
3.5	(a) Edge energy dispersion at $W=200$ nm and $V=0$ meV. (b) The dependence of energy gap on the width of system. . . . .	35

LIST OF FIGURES

---

3.6	(a) plotting of analytical result for the limited case semi-infinite. (b) Comparison of analytical result for limit case and numerical result for the case of the width is large enough. . . . .	36
3.7	Comparing the result of edge states in the two approaches. The parameters are $W=300$ , $V=0$ . . . . .	37
4.1	The two split gates system with electric potentials are applied at transverse boundaries. . . . .	39
4.2	Comparison of energy dispersion of the system in chapter 3 and the new system (a) $d=0$ for the new system and $V=0$ for the old system. (b) $d=W/2$ , $V=10$ for the new system and $V=10$ for the old system. Here $W=200\text{nm}$ . . . . .	42
4.3	The difference in the energy dispersion when we change potentials. (a) $V=10\text{meV}$ . (b) $V=30\text{meV}$ . (c) $V=-10\text{meV}$ . (d) $V=-20\text{meV}$ . Here $W=200\text{nm}$ . . . . .	43
4.4	Density of wave functions for down bands, with the case $V=0$ . Here $W=200\text{nm}$ . . . . .	44
4.5	(a) edge states (1st down level) at $k_x = 0$ under the change of potential. The consideration is in the HgTe/CdTe bar system in chapter 3. (b) Edge states (1st down level) at $k_x = 0$ under the change of potentials. The consideration is in the new HgTe/CdTe bar system . . . . .	44
5.1	The quantum transport model based on the HgTe/CdTe topological insulator material. . . . .	48
5.2	Conductance of the system for the special case $d=W/2$ . Other parameters are $W=200\text{nm}$ , $\ell=100$ , $V=15\text{meV}$ . . . . .	55
5.3	Conductance of the system. $W=200\text{nm}$ , $d=20\text{nm}$ , $\ell =100\text{nm}$ , $V=15\text{meV}$ . . . . .	56
5.4	Transmission in 2D HgTe/CdTe system with 1 interface, $V=10\text{meV}$ . No resonance states. . . . .	56



LIST OF FIGURES

---

5.5 Transmission in 2D HgTe/CdTe system with 2 interfaces,  $V=10\text{meV}$ ,  $\ell$   
 $=100\text{nm}$ . Some broad resonance states appear. . . . . 57



# Chapter 1

## Introduction

### 1.1 Background

#### 1.1.1 Topological insulator(TI).

- What is TI?

Topological insulators are new states of quantum matter. It is very different from traditionally defined metals and insulators. The electronic state of its body is an insulator with an energy gap, and its surface is metal state without energy gap. This surface metallic state, which is gapless, is also very different from the surface state in the general sense. The latter is due to dangling bonds on the surface or due to surface reconstruction. However, the surface state of topological insulator is completely determined by the topological structure of the bulk electronic states of the material. It is determined by symmetry, and independent from specific structure of the surface. Just because the surface metal state is determined by symmetry, it is very stable, almost not affected by impurity and disordering in the material. In addition, the basic property of topological insulator is the combined result of quantum mechanics and the theory of relativity. Due to the effect of spin orbit coupling, and under appropriate conditions, a surface electronic state of zero energy gap will form. This state is protected by the time reversal symmetry so that the state is robust against normal impurities.

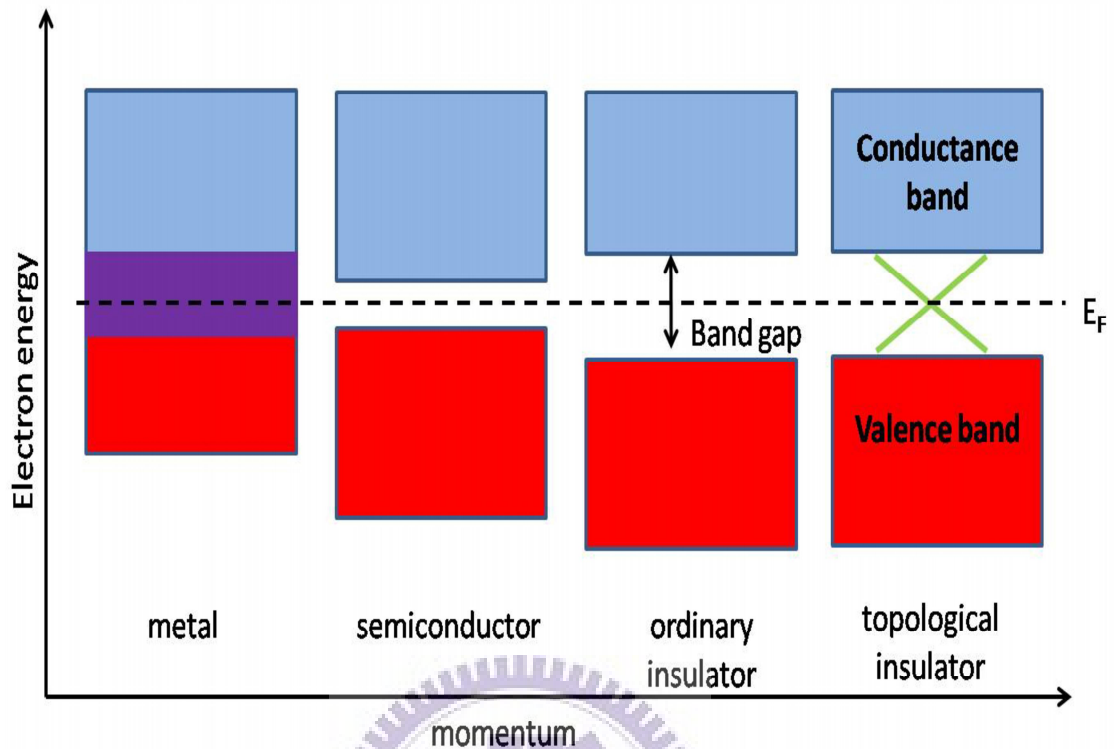


Figure 1.1: Electric band.

- What is different between TI and others material?

We can easily see the difference between materials by the band theory: Look at the figure 1.1, we see that metals contain a band that is partly empty and partly filled regardless of temperature. Therefore they have very high conductivity. It is not the same as metals, both ordinary insulators and semiconductors have an energy band where all states are occupied (the valence band) and a band of higher energy where all states are empty (the conduction band). The difference between an ordinary insulator and a semiconductor is just the size of the band gap between the valence band and the conduction band. In an ordinary insulator, the gap is large enough so that in an ordinary situation, the electrons will never gain energy enough to move up to the conduction band. The gap in a semiconductor is smaller, making the jump to the conduction. Topological insulators resemble an ordinary band insulator, with the Fermi level falling between the conduction and valence bands. On the surface of a topological insulator appear special states that fall within the bulk energy gap and allow surface metallic conduction band for the electrons

possible. These states are called surface states (in 3D) or edge states (in 2D).

- Why its name is "**topological insulator**" ?

Topological insulator with two meaning:

+ It behaves as an insulator in bulk band. So it has name "insulator".

+ To distinguish it from the ordinary insulator. Topological insulators are different from ordinary insulators on the topological properties. One sees that, the topological invariant, what characterized by TKNN number (or first Chern number) of topological insulator is integer number, while the ordinary insulator 's is zero.

- Features of topological insulators: In general, the features of topological insulators can identified as:

+ About conductance: Metal > semiconductor > **topological insulator** > ordinary insulator.

+ Comparing with the ordinary insulator:

\* The same bulk states, besides it has new states which locate at surfaces.

\* The  $Z_2$  invariant of topological insulator is  $\neq 0$ .

The  $Z_2$  invariant of ordinary insulator is  $= 0$ .

- Applications of this material?

The application to spintronics is an obvious one because the fact that surface conduction bands flowing in opposite directions are spin polarized. Also, the flow of electrons across the surface of a topological insulator does not dissipate energy as heat. This dissipatedness conduction has obvious application in small electronic devices because the conduction does not depend upon the size of the material.

## 1.1.2 Time reversal symmetry

- What is time reversal symmetry

Time reversal symmetry is known as symmetry that the forward-in -time behavior of solution is typically very similar to the backward-in-time behavior.

This concept can be described by equation:  $[H, \Theta] = 0$  with  $\Theta$  is the time reversal

symmetry operator.

$$H\psi(\vec{r}, t) = E.\psi(\vec{r}, t). \quad (1.1)$$

Under the action of time reversal operator, we have:

$$\Theta H\psi(\vec{r}, t) = E.\psi(\vec{r}, -t).$$

So clearly that solution is the same when we reversed time.

In a system which includes them time reversal symmetry, we always have double degeneracy (Kramer degeneracy) because if  $H|n\rangle = E_n|n\rangle$  then  $|n\rangle$  and  $\Theta|n\rangle$  belong the same energy eigenvalue  $E_n$ .

- How it effects to topological insulator?

To understand why time reversal symmetry is important for a topological insulator we consider the surface state characteristics. The surface states of a quantum topological insulator are spin polarized based upon the direction in which current is flowing. Time reversal symmetry acts on the wave vector  $\Theta u(\vec{k}) = -u(-\vec{k})$  and the spin  $\Theta\chi(\frac{1}{2}) = \chi(-\frac{1}{2})$ .

The surface states are time reversal invariant because spin and momentum are both negative under time reversal. The fact that the surface states are time reversal invariant makes them robust against perturbations that are time reversal invariant. However, a time reversal symmetry breaking perturbation like a magnetic field will destroy the surface states of a topological insulator.

### 1.1.3 Spin-orbit interaction.

Spin-orbit interaction (or spin-orbit coupling) is interaction of a particle's spin and its motion. A well know example of this effect is the shift in an electron's atomic energy level due to electromagnetic interaction between electron's spin and the magnetic field.

The spin-orbit interaction in vacuum can be written as:

$$H_{SO} = \frac{e\hbar}{4m_0^2.c^2} \cdot \vec{\sigma} \left( \vec{E} \times \vec{p} \right) = \lambda \vec{L} \vec{S}. \quad (1.2)$$

The physical mechanism of  $H_{SO}$  can be interpreted: an electron moving in an electric potential region sees, in its frame of reference, an effective magnetic field which couples with the electron spin through the magnetic moment of the electron spin. Through this effective magnetic field, which certainly depends on the orbital motion of the electron, the SOI is established.

- The role of SIO in topological insulator:

One sees that, nonmagnetic insulators without spin orbit interaction are ordinary insulators, and when the spin-orbit interaction becomes stronger, insulators may become topological insulators. Hence the edge states (or surface states) of topological insulators arise from the spin-orbit interaction. The spin-orbit interaction acts as a "spin-dependent magnetic field" and it gives rise to spin-dependent quantum Hall effect. The edge states from this spin-dependent quantum Hall effect consist of counter-propagating states with opposite spin. And therefore, they are called helical edge states.

#### 1.1.4 Hall effects.

We know that there are 4 kinds of Hall effects.

- Classical Hall effect is discovered by Edwin Hall in 1879. In the classical Hall effect, a voltage difference is produced across an electrical conductor and a magnetic field perpendicular to the current.

- Quantum Hall effect is the quantum version of the classical Hall effect. One observed this effect in two-dimensional electron systems, subjected to low temperatures and strong magnetic fields.

Hall conductivity is now quantized as:

$$\sigma_{xy} = N \cdot \frac{e^2}{h}$$

If  $N$  are integer numbers ( $N=1,2,3,\dots$ ), we have integer quantum Hall effect. If  $N$  are rational fraction ( $N=1/3,2/5,3/7,\dots$ ), we have the fractional quantum Hall effect.

- Spin Hall effect is accumulation of spin on the lateral surfaces of a current-carrying sample, the signs of the spin directions being opposite on the opposing boundaries. When the current direction is reversed, the directions of spin orientation is also reversed. Notice that, we do not need a magnetic field in this case. If we apply a strong enough magnetic field is applied in the direction perpendicular to the orientation of the spins at the surfaces, SHE will disappear because of the spin precession around the direction of the magnetic field.

- The quantum spin Hall state is a state of matter proposed to exist in special, two-dimensional, semiconductors with spin-orbit coupling. The quantum spin Hall state of matter is the cousin of the integer quantum Hall state, but, unlike the latter, it does not require the application of a large magnetic field. The quantum spin Hall state does not break any discrete symmetries (such as time-reversal or parity). The first proposal for the existence of a quantum spin Hall state was developed by Kane and Mele[8] who adapted an earlier model for graphene by F. Duncan M. Haldane[11] which exhibits an integer quantum Hall effect. The Kane and Mele model is two copies of the Haldane model such that the spin up electron exhibits a chiral integer quantum Hall Effect while the spin down electron exhibits an anti-chiral integer quantum Hall effect. It has been recently proposed [10] and subsequently experimentally realized in mercury (II) telluride (HgTe/CdTe) semiconductors.

Overall the Kane-Mele model has a charge-Hall conductance of exactly zero but a spin-Hall conductance of exactly  $\sigma_{xy}^{spin} = 2$  (in units of  $\frac{e^2}{4\pi}$ ). Independently, a quantum spin Hall model was proposed by Bernevig and Zhang[9] in an intricate strain architec-

ture which engineers, due to spin-orbit coupling, a magnetic field pointing upwards for spin-up electrons and a magnetic field pointing downwards for spin-down electrons. The main ingredient is the existence of spin-orbit coupling, which can be understood as a momentum-dependent magnetic field coupling to the spin of the electron.

Strictly speaking, the models with spin-orbit coupling do not have a quantized spin Hall conductance  $\sigma_{xy}^{spin} \neq 2$ . Those models are more properly referred as topological insulator which is an example of topologically ordered states.

## 1.2 Motivation.

- Introducing to 2D topological insulator HgTe/CdTe:

The two dimensional incarnation of the topological insulator states, also known as the quantum spin Hall effect was first predicted to be present in graphene, by Kane and Mele [8]. However, one sees that the spin-orbit interaction in graphene is too weak to produce a band large enough. It was later in 2006 proposed by Bernevig, Hughes and Zhang [10] to be present in mercury telluride (HgTe/CdTe) quantum wells which were also demonstrated by König in 2007 [7].

Mercury telluride quantum wells can be prepared by sandwiching the material between cadmium telluride, which has a similar lattice constant but much weaker spin-orbit coupling. Therefore, increasing the thickness  $d$  of the HgTe/CdTe layer increases the strength of the spin-orbit coupling for the entire quantum well. For a thin quantum well, as shown in the left of the figure 1.2, the CdTe has the dominant effect and the bands have a normal ordering: The s-like (electron in s orbital) conduction subband E1 is located above the p-like (electron in p orbital) valence subband H1. In a thick quantum well as shown on the right of the figure, the opposite ordering occurs due to the increase of thickness  $d$  of the HgTe/CdTe layer.

The two dimensional topological insulator mercury telluride can be described by an



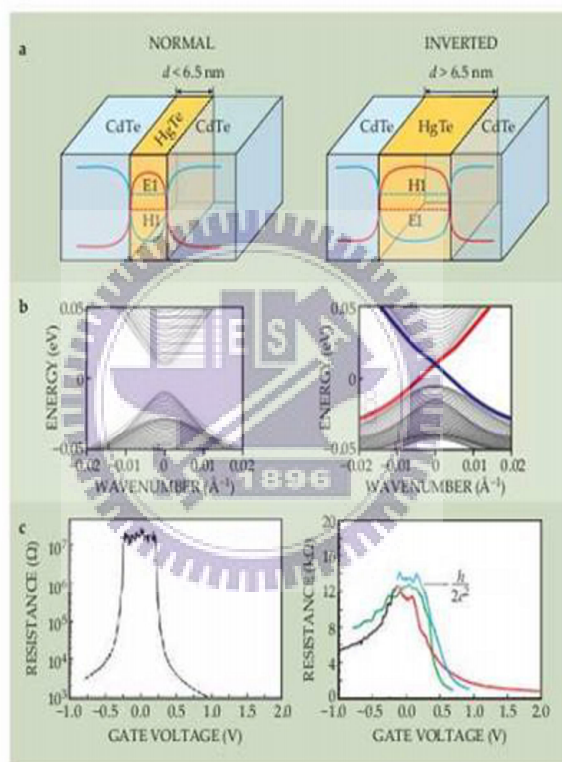


Figure 1.2: HgTe/CdTe quantum well at thickness greater than and less than the critical thickness.

effective Hamiltonian [10]:

$$H(\vec{k}) = \varepsilon(\vec{k}) + \begin{pmatrix} M_k & Ak_- & 0 & 0 \\ Ak_+ & -M_k & 0 & 0 \\ 0 & 0 & M_k & -Ak_- \\ 0 & 0 & -Ak_+ & -M_k \end{pmatrix} \quad (1.3)$$

$$\varepsilon(\vec{k}) = C - Dk^2, M_k = M - Bk^2.$$

Where the upper 2x2 block describes spin-up electrons in the s-like  $E_1$  conduction and the p-like  $H_1$  valence bands, and the lower block describes the spin-down electrons in those bands. The term  $\varepsilon(\vec{k})$  is an unimportant bending of all bands. The energy gap between the bulk bands is  $2M$ . And  $B$  typically negative, describes the curvature of the bands;  $A$  incorporates interband coupling to lowest order. For  $M/B < 0$ , the eigen states of model describe a trivial insulator. For thickness quantum wells, the band are inverted,  $M$  becomes negative and we have topological insulators.

In our research, we do work with the values of the parameters  $A, B, C, D, M$  at the thickness of the HgTe/CdTe quantum well is  $d_{qw} = 7nm$ . And therefore,  $A = 346.5 meV.nm$ ,  $B = -686 meV.nm^2$ ,  $C = 0$ ,  $D = -512 meV.nm^2$ ,  $M = -10 meV$ .

- Recently, some interesting research on HgTe/CdTe were shown [2],[4],[5],[6]. In these papers, they considered the system of HgTe/CdTe quantum spin Hall bar without external fields or under the electric field which is filled in the system.

Because the edge states are the feature states of the 2D topological insulator. So we do not want to apply a electric field for the whole system. We propose to apply electric potentials at transverse boundaries only. And then we have the two split gates system (figure 1.3).

When we do that, we mean the edge states will be effected by potentials much more than to bulk states. And so we can control edge states by the electric potentials. If potentials are large enough, the edge states will be destroyed around  $\Gamma$  point. From this

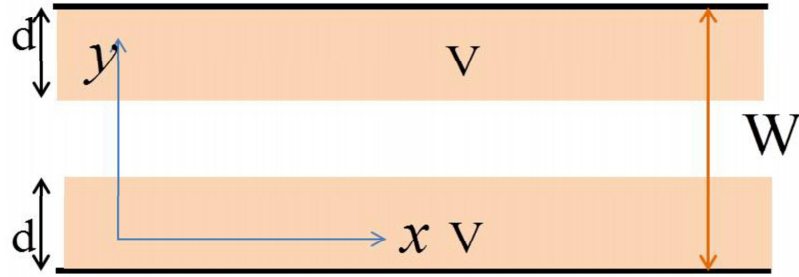


Figure 1.3: The two split gates system: HgTe/CdTe bar with electric potentials are applied at transverse boundaries.

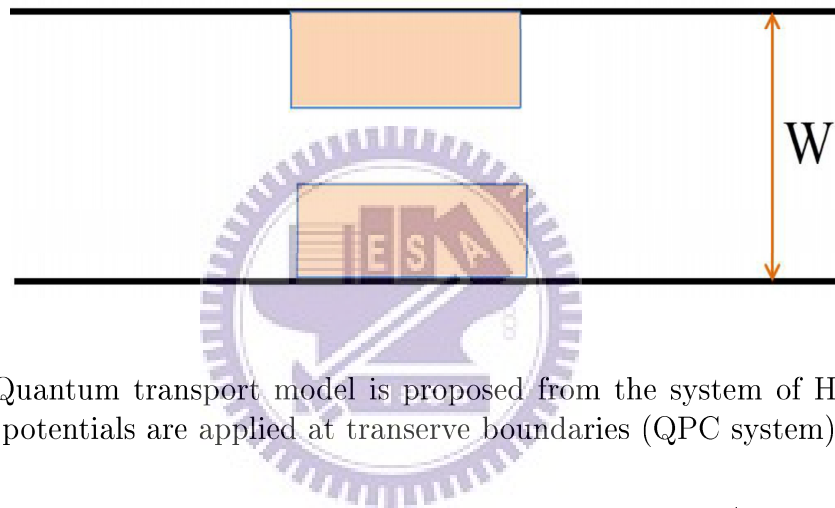


Figure 1.4: Quantum transport model is proposed from the system of HgTe/CdTe bar with electric potentials are applied at transverse boundaries (QPC system).

idea, we also proposed a quantum transport system on the HgTe/CdTe material like in the figure 1.4.

This transport system looks like quantum point contact (QPC). Because we can control the edge states in the middle region, so thank to the voltage gates, we can control the current of edge states, and therefore change the conductance of the system.

When the width of the potentials areas equal 0 or  $W/2$ . Our system closes to the HgTe/CdTe quantum spin Hall bar. And we can check our result via the papers which have been published.


### 1.3 A guiding tour to the thesis.

This thesis includes 6 chapters. In chapter 1, we already introduced topological insulators. In chapter 2, we will work out the topological features of HgTe/CdTe materials. Berry curvature and Chern number will be calculated and analyzed. In chapter 3, we would like to present the calculation and the result for the HgTe/CdTe bar system. Two approaches will be presented and we can compare the results with result of other papers. In chapter 4, we study the two split gates system. From here we can see the effect of potentials to the edge states. In chapter 5, we go to the quantum transport system which we proposed early. And in chapter 6, it is our conclusions for this research. Besides, we also propose an idea as a future work.



## Chapter 2

# Study topological features of HgTe/CdTe material via Berry curvature and Chern number.



HgTe/CdTe is a 2D topological insulator, so it must be different from ordinary insulators. The difference of topological insulators and ordinary insulators are in the topology of space of wave functions. For topological insulators, one sees that the topological invariant is different from 0. While the topological invariant of ordinary insulators is equal to 0. In physics, the topological properties normally are considered under the change of Berry curvature. For 2D topological insulators (also are quantum spin hall insulator), they are distinguished from the ordinary insulators by  $Z_2$  invariant, which can be calculated from Chern numbers. Chern numbers will be integrated from the Berry curvature over the Brillouin zone. In this chapter, we will study the topological properties of HgTe/CdTe materials to see they are really 2D topological insulators.

First, we can reduce our work on the 2x2 matrix Hamiltonian instead of 4x4 Hamiltonian, which was introduced in the reference [10] as well as in chapter 1. Why can we do that?

If we set the general form of wave function like this  $\psi(x, y) = \begin{pmatrix} \Phi(x, y) \\ \Phi'(x, y) \end{pmatrix}$ .

Then the Schrodinger equation can be simple as

$$\begin{pmatrix} H(k) & 0 \\ 0 & H^*(-k) \end{pmatrix} \begin{pmatrix} \Phi(x, y) \\ \Phi'(x, y) \end{pmatrix} = E \begin{pmatrix} \Phi(x, y) \\ \Phi'(x, y) \end{pmatrix} \Leftrightarrow \begin{cases} H(k)\Phi(x, y) = E\Phi(x, y) \\ H^*(-k)\Phi'(x, y) = E\Phi'(x, y) \end{cases}$$

This result says that we just need to solve the equation  $H(k)\Phi(x, y) = E\Phi(x, y)$ . The other solution we can reduce from this solution because of relation between  $H(k)$  and  $H^*(-k)$ . This relation is time reversal symmetry. So, we just solve Schrodinger equation with the upper block (spin up) and employ the time reversal symmetry to get the results for the lower block (spin down).

## 2.1 Berry phase and Berry curvature.

### 2.1.1 Overview of Berry phase and Berry curvature.

In physics, Berry connection and Berry curvature are related concepts, which can be viewed, respectively, as a local gauge potential and gauge field associated with the Berry phase. These concepts were introduced by Michael Berry in a paper published in 1984[12] emphasizing how geometric phases provide a powerful unifying concept in several branches of classical and quantum physics. Such phases have come to be known as Berry phases [12], [13].

In a cyclic adiabatic evolution, if the n-th eigenvalue  $\varepsilon_n(\vec{k})$  remains non-degenerate everywhere along the path and the variation with time t is sufficiently slow, then a system initially in the eigenstate  $|u_{\vec{k}(0),n}\rangle$  will remain in an instantaneous eigenstate  $|u_{\vec{k}(t),n}\rangle$ ,

up to a phase

$$\gamma_n(t) = i \int_{\vec{k}(0)}^{\vec{k}(t)} d\vec{k} \cdot \left\langle u_{\vec{k},n} \left| \frac{d}{d\vec{k}} \right| u_{\vec{k},n} \right\rangle \quad (2.1)$$

With  $\gamma_n(t)$  being the Berry phase. Notice that the integral is working on a closed path  $k(t) = k(0)$  of the cyclic evolution.

$$\text{Using the Stoke's theorem, we get } \gamma_n = i \int dS \cdot \nabla_{\vec{k}} \times \left\langle u_{\vec{k},n} \left| \nabla_{\vec{k}} u_{\vec{k},n} \right. \right\rangle = \int dS \cdot \Omega_n(\vec{k})$$

Where

$$\Omega_n(\vec{k}) = i \nabla_{\vec{k}} \times \left\langle u_{\vec{k},n} \left| \nabla_{\vec{k}} u_{\vec{k},n} \right. \right\rangle \quad (2.2)$$

is called the Berry curvature.

For numerical calculation, one sees that the formula (2.2) is not convenient and has some difficulties on the technical calculations. So, with demand for calculation one tried to transform (2.2) to another form which can help us to calculate more easily. Let rewrite (2.2) as follow

$$\begin{aligned} \Omega_n(\vec{k}) &= i \nabla_{\vec{k}} \times \left\langle u_{\vec{k},n} \left| \nabla_{\vec{k}} u_{\vec{k},n} \right. \right\rangle \\ &= i \left[ \left\langle \nabla_{\vec{k}} u_{\vec{k},n} \left| \times \right| \nabla_{\vec{k}} u_{\vec{k},n} \right\rangle + \left\langle u_{\vec{k},n} \left| \nabla_{\vec{k}} \times \nabla_{\vec{k}} u_{\vec{k},n} \right. \right\rangle \right] = i \left\langle \nabla_{\vec{k}} u_{\vec{k},n} \left| \times \right| \nabla_{\vec{k}} u_{\vec{k},n} \right\rangle \end{aligned}$$

For example we consider along z direction, so  $\Omega_n(\vec{k}) = i \cdot \left[ \left\langle \frac{\partial u_{\vec{k},n}}{\partial k_x} \left| \frac{\partial u_{\vec{k},n}}{\partial k_y} \right. \right\rangle - \left\langle \frac{\partial u_{\vec{k},n}}{\partial k_y} \left| \frac{\partial u_{\vec{k},n}}{\partial k_x} \right. \right\rangle \right]$ .

Inserting the complete set  $\sum_{n'} \left| u_{\vec{k},n'} \right\rangle \left\langle u_{\vec{k},n'} \right| = 1$  into the above result, we have

$$\Omega_n(\vec{k}) = i \cdot \sum_{n'} \left[ \left\langle \frac{\partial u_{\vec{k},n}}{\partial k_x} \left| u_{\vec{k},n'} \right. \right\rangle \cdot \left\langle u_{\vec{k},n'} \left| \frac{\partial u_{\vec{k},n}}{\partial k_y} \right. \right\rangle - \left\langle \frac{\partial u_{\vec{k},n}}{\partial k_y} \left| u_{\vec{k},n'} \right. \right\rangle \cdot \left\langle u_{\vec{k},n'} \left| \frac{\partial u_{\vec{k},n}}{\partial k_x} \right. \right\rangle \right]$$

Considering  $\langle u_{\vec{k},n'}^{\rightarrow} | \nabla_{\vec{k}} H | u_{\vec{k},n}^{\rightarrow} \rangle$

$$\begin{aligned}
 \langle u_{\vec{k},n'}^{\rightarrow} | \nabla_{\vec{k}} H | u_{\vec{k},n}^{\rightarrow} \rangle &= \langle u_{\vec{k},n'}^{\rightarrow} | \nabla_{\vec{k}} (H | u_{\vec{k},n}^{\rightarrow} \rangle) - \langle u_{\vec{k},n'}^{\rightarrow} | H (\nabla_{\vec{k}} | u_{\vec{k},n}^{\rightarrow} \rangle) \\
 &= \langle u_{\vec{k},n'}^{\rightarrow} | \nabla_{\vec{k}} (E_{\vec{k},n}^{\rightarrow} | u_{\vec{k},n}^{\rightarrow} \rangle) - \langle u_{\vec{k},n'}^{\rightarrow} | E_{\vec{k},n'}^{\rightarrow} (\nabla_{\vec{k}} | u_{\vec{k},n}^{\rightarrow} \rangle) \\
 &= (\nabla_{\vec{k}} E_{\vec{k},n}^{\rightarrow}) \langle u_{\vec{k},n'}^{\rightarrow} | u_{\vec{k},n}^{\rightarrow} \rangle + E_{\vec{k},n}^{\rightarrow} \langle u_{\vec{k},n'}^{\rightarrow} | \nabla_{\vec{k}} u_{\vec{k},n}^{\rightarrow} \rangle - E_{\vec{k},n'}^{\rightarrow} \langle u_{\vec{k},n'}^{\rightarrow} | \nabla_{\vec{k}} | u_{\vec{k},n}^{\rightarrow} \rangle \\
 &= (\nabla_{\vec{k}} E_{\vec{k},n}^{\rightarrow}) \cdot 0 + E_{\vec{k},n}^{\rightarrow} \langle u_{\vec{k},n'}^{\rightarrow} | \nabla_{\vec{k}} u_{\vec{k},n}^{\rightarrow} \rangle - E_{\vec{k},n'}^{\rightarrow} \langle u_{\vec{k},n'}^{\rightarrow} | \nabla_{\vec{k}} | u_{\vec{k},n}^{\rightarrow} \rangle \\
 &= (E_{\vec{k},n}^{\rightarrow} - E_{\vec{k},n'}^{\rightarrow}) \langle u_{\vec{k},n'}^{\rightarrow} | \nabla_{\vec{k}} u_{\vec{k},n}^{\rightarrow} \rangle \\
 \Rightarrow \langle u_{\vec{k},n'}^{\rightarrow} | \nabla_{\vec{k}} u_{\vec{k},n}^{\rightarrow} \rangle &= \frac{\langle u_{\vec{k},n'}^{\rightarrow} | \nabla_{\vec{k}} H | u_{\vec{k},n}^{\rightarrow} \rangle}{(E_{\vec{k},n}^{\rightarrow} - E_{\vec{k},n'}^{\rightarrow})} \text{ for } n' \neq n \\
 \Rightarrow \Omega_n(\vec{k}) &= i \cdot \sum_{n' \neq n} \left[ \frac{\langle u_{\vec{k},n}^{\rightarrow} | \partial_{k_x} H | u_{\vec{k},n'}^{\rightarrow} \rangle \langle u_{\vec{k},n'}^{\rightarrow} | \partial_{k_y} H | u_{\vec{k},n}^{\rightarrow} \rangle}{(E_{\vec{k},n}^{\rightarrow} - E_{\vec{k},n'}^{\rightarrow})^2} \right. \\
 &\quad \left. \frac{\langle u_{\vec{k},n}^{\rightarrow} | \partial_{k_y} H | u_{\vec{k},n'}^{\rightarrow} \rangle \langle u_{\vec{k},n'}^{\rightarrow} | \partial_{k_x} H | u_{\vec{k},n}^{\rightarrow} \rangle}{(E_{\vec{k},n}^{\rightarrow} - E_{\vec{k},n'}^{\rightarrow})^2} \right] \tag{2.3}
 \end{aligned}$$

Or we can simply write as

$$\Omega_n(\vec{k}) = i \cdot \sum_{n' \neq n} \left[ \frac{(k_x \because k_y) - (k_y \because k_x)}{(E_{\vec{k},n}^{\rightarrow} - E_{\vec{k},n'}^{\rightarrow})^2} \right] \tag{2.4}$$

Where

$$\begin{aligned}
 (k_x \because k_y) &= \langle u_{\vec{k},n}^{\rightarrow} | \partial_{k_x} H | u_{\vec{k},n'}^{\rightarrow} \rangle \langle u_{\vec{k},n'}^{\rightarrow} | \partial_{k_y} H | u_{\vec{k},n}^{\rightarrow} \rangle \\
 (k_y \because k_x) &= \langle u_{\vec{k},n}^{\rightarrow} | \partial_{k_y} H | u_{\vec{k},n'}^{\rightarrow} \rangle \langle u_{\vec{k},n'}^{\rightarrow} | \partial_{k_x} H | u_{\vec{k},n}^{\rightarrow} \rangle
 \end{aligned}$$

### 2.1.2 The Berry curvature in HgTe/CdTe topological insulators.

To calculate the Berry curvature, we need to know Eigen states and Eigen energies of the Hamiltonian. So, first we will start from the Schrodinger equation to find these



things. From the equation  $Hu = Eu$  we have

$$\begin{pmatrix} C + V - D_+.(k_x^2 + k_y^2) + M & A.(k_x - ik_y) \\ A.(k_x + ik_y) & C + V - D_-.(k_x^2 + k_y^2) - M \end{pmatrix} \begin{pmatrix} a \\ b \end{pmatrix} = E \begin{pmatrix} a \\ b \end{pmatrix} \quad (2.5)$$

Solving this equation we will get both solutions for  $E$  and  $u$ . First of all, we move  $E.u$  to the left hand side and we get the equation  $(H - 1.E)u = 0$ . Directly we have  $\det(H - 1.E) = 0$ . Because the matrix is 2x2, so we get 2 roots for  $E$ .

$$E = C + V - Dk^2 \pm \sqrt{(Bk^2 - M)^2 + A^2.k^2} \quad (2.6)$$

Let denote

$$E_1 = C + V - Dk^2 + \sqrt{(Bk^2 - M)^2 + A^2.k^2}, E_{-1} = C + V - Dk^2 - \sqrt{(Bk^2 - M)^2 + A^2.k^2}$$

Inserting (2.6) back into the (2.5) we will see the relation between a and b as following

$$a = \frac{A.k_-}{B.k^2 - M \pm \sqrt{(Bk^2 - M)^2 + A^2.k^2}}.b \quad (2.7)$$

And thus we have 2 Eigen vectors. They must be in forms

$$\begin{cases} u_1 = \begin{pmatrix} a_1 \\ b_1 \end{pmatrix} = c_1 \cdot \begin{pmatrix} A.k_- \\ B.k^2 - M + \sqrt{(Bk^2 - M)^2 + A^2.k^2} \end{pmatrix} \\ u_{-1} = \begin{pmatrix} a_{-1} \\ b_{-1} \end{pmatrix} = c_{-1} \cdot \begin{pmatrix} A.k_- \\ B.k^2 - M - \sqrt{(Bk^2 - M)^2 + A^2.k^2} \end{pmatrix} \end{cases} \quad (2.8)$$

The Eigen vector  $u_1$  is corresponding to  $E_1$  and  $u_{-1}$  is corresponding to  $E_{-1}$ . a and b can be found more specifically by the normalized condition  $|a|^2 + |b|^2 = 1$ . Since we can

know that

$$b^2 = \frac{\sqrt{(Bk^2 - M)^2 + A^2.k^2} \pm (B.k^2 - M)^2}{2\sqrt{(Bk^2 - M)^2 + A^2.k^2}} \quad (2.9)$$

Now we can start to calculate the Berry curvature based on the formula (2.4). First, noting that

$$\partial k_- / \partial k_x = \partial(k_x - i.k_y) / \partial k_x = 1; \partial k_- / \partial k_y = -i \quad \text{and} \quad \partial k / \partial k_x = k_x / k; \partial k / \partial k_y = k_y / k$$

, so we get

$$\begin{aligned} \partial_{k_x} H &= \begin{pmatrix} -2D_+.k_x & A \\ A & -2D_-.k_x \end{pmatrix} = -2k_x D - 2k_x B. \begin{pmatrix} 1 & 0 \\ 0 & -1 \end{pmatrix} + A. \begin{pmatrix} 0 & 1 \\ 1 & 0 \end{pmatrix} \\ \partial_{k_y} H &= \begin{pmatrix} -2D_+.k_y & -iA \\ iA & -2D_-.k_y \end{pmatrix} = -2k_y D - 2k_y B. \begin{pmatrix} 1 & 0 \\ 0 & -1 \end{pmatrix} + iA. \begin{pmatrix} 0 & -1 \\ 1 & 0 \end{pmatrix} \end{aligned}$$

We only have 2 states, so we do not need to take summation in (2.4), and the index n is indicated for 1 or -1. The denominator is always equal to  $(E_1 - E_{-1})^2 = (E_{-1} - E_1)^2 = \left(2\sqrt{(Bk^2 - M)^2 + A^2.k^2}\right)^2$ . And we go to a better form

$$\Omega_n(\vec{k}) = i \frac{(k_x :: k_y) - (k_y :: k_x)}{\left(2\sqrt{(Bk^2 - M)^2 + A^2.k^2}\right)^2}. \quad (2.10)$$

Let consider the first term of the numerator.

$$(k_x :: k_y) = \langle u_n(k) | \partial_{k_x} H | u_{-n}(k) \rangle \cdot \langle u_{-n}(k) | \partial_{k_y} H | u_n(k) \rangle$$

$$\begin{aligned}
\langle u_n(k) | \partial_{k_x} H | u_{-n}(k) \rangle &= \begin{pmatrix} a_n^* & b_n^* \end{pmatrix} \left[ -2k_x \begin{pmatrix} D_+ & 0 \\ 0 & D_- \end{pmatrix} + A \begin{pmatrix} 0 & 1 \\ 1 & 0 \end{pmatrix} \right] \begin{pmatrix} a_{-n} \\ b_{-n} \end{pmatrix} \\
&= -2k_x \cdot (D_+ a_n^* \cdot a_{-n} + D_- b_n^* \cdot b_{-n}) + A \cdot (a_n^* \cdot b_{-n} + b_n^* \cdot a_{-n}) \\
&= -2k_x \cdot X + A \cdot (a_n^* \cdot b_{-n} + b_n^* \cdot a_{-n}) \\
\langle u_{-n}(k) | \partial_{k_y} H | u_n(k) \rangle &= \begin{pmatrix} a_{-n}^* & b_{-n}^* \end{pmatrix} \left[ -2k_y \begin{pmatrix} D_+ & 0 \\ 0 & D_- \end{pmatrix} + iA \begin{pmatrix} 0 & -1 \\ 1 & 0 \end{pmatrix} \right] \begin{pmatrix} a_n \\ b_n \end{pmatrix} \\
&= -2k_y \cdot (D_+ a_{-n}^* \cdot a_n + D_- b_{-n}^* \cdot b_n) + iA \cdot (-a_{-n}^* \cdot b_n + b_{-n}^* \cdot a_n) \\
&= -2k_y \cdot X + iA \cdot (-a_{-n}^* \cdot b_n + b_{-n}^* \cdot a_n)
\end{aligned}$$

Where

$$X = (D_+ a_n^* \cdot a_{-n} + D_- b_n^* \cdot b_{-n}). \quad (2.11)$$

$$\begin{aligned}
(k_x \because k_y) &= [-2k_x \cdot X + A \cdot (a_n^* \cdot b_{-n} + b_n^* \cdot a_{-n})] \cdot [-2k_y \cdot X + iA \cdot (-a_{-n}^* \cdot b_n + b_{-n}^* \cdot a_n)] \\
&= 4k_x k_y X^2 - 2ik_x \cdot XA \cdot (-a_{-n}^* \cdot b_n + b_{-n}^* \cdot a_n) - 2k_y \cdot XA \cdot (a_n^* \cdot b_{-n} + b_n^* \cdot a_{-n}) \\
&\quad + iA^2 (-a_n^* \cdot b_n a_n^* \cdot b_n + b_n^* \cdot a_n a_n^* \cdot b_n - a_n^* \cdot b_n b_n^* \cdot a_n + b_n^* \cdot a_n b_n^* \cdot a_n)
\end{aligned} \quad (2.12)$$

Doing in similar way for the second term of numerator, we have

$$\begin{aligned}
(k_y \because k_x) &= \langle u_n(k) | \partial_{k_y} H | u_{-n}(k) \rangle \langle u_{-n}(k) | \partial_{k_x} H | u_n(k) \rangle \\
&= 4k_x k_y X^2 - 2k_y \cdot XA \cdot (a_n^* \cdot b_n + b_n^* \cdot a_n) - 2ik_x \cdot XA \cdot (-a_n^* \cdot b_n + b_n^* \cdot a_n) \\
&\quad + iA^2 (-a_n^* \cdot b_n a_n^* \cdot b_n - a_n^* \cdot b_n b_n^* \cdot a_n + b_n^* \cdot a_n a_n^* \cdot b_n + b_n^* \cdot a_n b_n^* \cdot a_n)
\end{aligned} \quad (2.13)$$

Substituting (2.12) and (2.13) into (2.10) we get result for the numerator of (2.10).

$$\begin{aligned}
 & (k_x :: k_y) - (k_y :: k_x) \\
 &= 2k_y.X.A. [b_n (a_{-n} * -a_{-n}) + b_{-n} (a_n - a_n^*)] + 2ik_x.XA. [b_n (a_{-n} * +a_{-n}) - b_{-n} (a_n + a_n^*)] \cdot \\
 &+ 2iA^2 (a_n a_n^* . b_{-n}^2 - a_{-n} a_{-n}^* . b_n^2)
 \end{aligned} \tag{2.14}$$

Notice that in the calculation we already consider  $b_n$  are positive quantities. To continuous to reduce this result, we need to use the relation (2.7) of  $a_n$  and  $b_n$  for next calculations.

First,

$$\begin{aligned}
 X &= (D_+ a_n^* . a_{-n} + D_- b_n^* . b_{-n}) \\
 &= D_+ \frac{A.k_+}{B.k^2 - M + n\sqrt{(Bk^2 - M)^2 + A^2.k^2}} . b_n . \frac{A.k_-}{B.k^2 - M - n\sqrt{(Bk^2 - M)^2 + A^2.k^2}} . b_{-n} + D_- b_n^* . b_{-n} \\
 &= D_+ \frac{A^2.k^2}{(Bk^2 - M)^2 - n^2[(Bk^2 - M)^2 + A^2.k^2]} . b_n . b_{-n} + D_- b_n . b_{-n} \\
 &= - (D_+ - D_-) b_n . b_{-n} \quad (\text{because } n^2 = 1) \\
 &= -2B . b_n b_{-n}.
 \end{aligned}$$

And, second

$$\begin{aligned}
 & [b_n (a_{-n} * -a_{-n}) + b_{-n} (a_n - a_n^*)] \\
 &= b_n \frac{A.2ik_y}{B.k^2 - M - n\sqrt{(Bk^2 - M)^2 + A^2.k^2}} . b_{-n} + b_{-n} \frac{-A.2ik_y}{B.k^2 - M + n\sqrt{(Bk^2 - M)^2 + A^2.k^2}} b_n \\
 &= 4iAk_y b_n b_{-n} \frac{n\sqrt{(Bk^2 - M)^2 + A^2.k^2}}{-A^2.k^2} \quad (n^2 = 1 \text{ is applied})
 \end{aligned}$$

$$\begin{aligned}
 & [b_n (a_{-n} * +a_{-n}) - b_{-n} (a_n + a_n^*)] \\
 &= b_n \frac{A.2k_x}{B.k^2 - M - n\sqrt{(Bk^2 - M)^2 + A^2.k^2}} . b_{-n} - b_{-n} \frac{A.2k_x}{B.k^2 - M + n\sqrt{(Bk^2 - M)^2 + A^2.k^2}} b_n \\
 &= 4Ak_x b_n b_{-n} \frac{n\sqrt{(Bk^2 - M)^2 + A^2.k^2}}{-A^2.k^2} \quad (n^2 = 1 \text{ is applied})
 \end{aligned}$$

CHAPTER 2. STUDY TOPOLOGICAL FEATURES OF HGTE/CDTE MATERIAL VIA BERRY CURVATURE AND CHERN NUMBER.

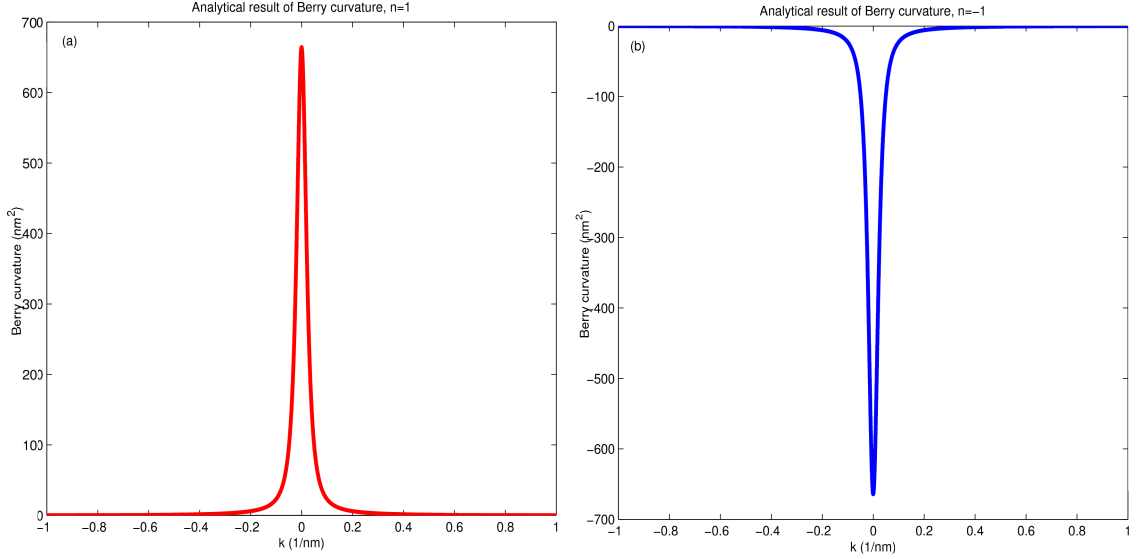


Figure 2.1: The plotting of the Berry curvature for analytical result.

The final term is

$$\begin{aligned}
 & (a_n a_n \cdot b_{-n}^2 - a_{-n} a_{-n} \cdot b_n^2) \\
 &= \frac{A^2 \cdot k^2}{(B \cdot k^2 - M + n \sqrt{(Bk^2 - M)^2 + A^2 \cdot k^2})^2} \cdot b_n^2 \cdot b_{-n}^2 - \frac{A^2 \cdot k^2}{(B \cdot k^2 - M - n \sqrt{(Bk^2 - M)^2 + A^2 \cdot k^2})^2} \cdot b_{-n}^2 \cdot b_n^2 \\
 &= -4A^2 \cdot k^2 b_n^2 \cdot b_{-n}^2 \frac{(B \cdot k^2 - M) \cdot n \sqrt{(Bk^2 - M)^2 + A^2 \cdot k^2}}{(-A^2 \cdot k^2)^2} \\
 &= 4b_n^2 \cdot b_{-n}^2 \frac{(B \cdot k^2 - M) \cdot n \sqrt{(Bk^2 - M)^2 + A^2 \cdot k^2}}{-A^2 \cdot k^2}
 \end{aligned}$$

Putting all in (2.14) and using the formula of  $b_n^2$  (2.9) we have

$$(k_x \cdot k_y) - (k_y \cdot k_x) = 2inA^2 \cdot \frac{(B \cdot k^2 + M)}{\sqrt{(Bk^2 - M)^2 + A^2 \cdot k^2}}.$$

And thus the Berry curvature now is ready calculated by (2.10)

$$\begin{aligned}
 \Omega_n(\vec{k}) &= i \frac{(k_x \cdot k_y) - (k_y \cdot k_x)}{(2\sqrt{(Bk^2 - M)^2 + A^2 \cdot k^2})^2} \\
 &= i \frac{2inA^2 \cdot \frac{(B \cdot k^2 + M)}{\sqrt{(Bk^2 - M)^2 + A^2 \cdot k^2}}}{(2\sqrt{(Bk^2 - M)^2 + A^2 \cdot k^2})^2} = -n \cdot \frac{A^2 (B \cdot k^2 + M)}{2[(Bk^2 - M)^2 + A^2 \cdot k^2]^{3/2}}
 \end{aligned} \tag{2.15}$$

## 2.2 Chern number.

Chern number is an important key to help us go to the  $Z_2$  invariant, which can help us to distinguish topological insulators and trivial insulators. Chern number can be calculated via the Berry curvature by the formula

$$C_n = \frac{1}{2\pi} \int d\vec{k} \cdot \Omega_n(\vec{k}). \quad (2.16)$$

Here we do work on the 2 dimensions momentum space. So  $d\vec{k} = dk_x dk_y = 2\pi k \cdot dk = \pi \cdot dk^2$

$$\Rightarrow C_n = \frac{1}{2} \int dk^2 \cdot \Omega_n(\vec{k}).$$

Now we can put the result of the Berry curvature in (2.15) in the above formula, in addition we notice that because the Berry curvature decays rapidly to 0. So we can change the boundaries of the integral on the first Brillouin zone to boundaries 0 and infinite of  $k$ , and we have

$$C_n = -\frac{1}{2} \int_0^\infty dk^2 \cdot n \cdot \frac{A^2 (B \cdot k^2 + M)}{2[(Bk^2 - M)^2 + A^2 \cdot k^2]^{3/2}}. \quad (2.17)$$

Setting

$$\cos\theta = \frac{(B \cdot k^2 - M)}{\sqrt{(Bk^2 - M)^2 + A^2 \cdot k^2}}. \quad (2.18)$$

We find the boundaries of the new variable as follow

$$k^2 = 0 \Rightarrow \theta = \theta_1; \cos\theta_1 = -\frac{M}{\sqrt{M^2}} = -\frac{M}{|M|} = -\text{sgn}(M)$$

$$k^2 = \infty \Rightarrow \theta = \theta_2 \quad \cos\theta_2 = \lim_{k \rightarrow \infty} \frac{(B \cdot k^2 - M)}{\sqrt{(Bk^2 - M)^2 + A^2 \cdot k^2}} = \frac{B}{\sqrt{(B)^2}} = \text{sgn}(B)$$

$$\frac{\partial \cos\theta}{\partial k^2} = \frac{A^2 (B.k^2 + M)}{2[(Bk^2 - M)^2 + A^2.k^2]^{3/2}}$$

So,  $C_n = -\frac{1}{2} \int_0^\infty dk^2 . n . \frac{\partial \cos\theta}{\partial k^2} = -\frac{1}{2} n (\cos\theta_2 - \cos\theta_1) = -\frac{1}{2} n [\text{sgn}(B) + \text{sgn}(M)]$ . In all our calculations, we use the value of parameters are  $B = -686$ ;  $M = -10$ .

$$\Rightarrow C_n = n.$$

$$\Rightarrow C_n = \begin{cases} 1 & \text{for } n = 1 : \text{conductance band.} \\ -1 & \text{for } n = -1 : \text{valence band.} \end{cases} \quad (2.19)$$

## 2.3 The analysis of the result of Berry curvature and Chern number.

### 2.3.1 The Berry curvature under the time reversal symmetry.

We know that the time reversal symmetry is an important property of quantum spin hall insulators. We know that, under the effect of the time reversal symmetry, momentum and spin change their sign.

For Berry curvature, the above results that we obtained are just for the upper block of the Hamiltonian, the block of spin up. What is result of Berry curvature for the spin down block?

We can answer this question by considering the change of the Berry curvature under the action of the time reversal operator.

First, we write the Berry curvature as follow

$$\Omega_n(\vec{k}) = i \nabla_{\vec{k}} \times \langle u_{\vec{k},n} | \nabla_{\vec{k}} u_{\vec{k},n} \rangle = \nabla_{\vec{k}} \times \vec{A}_{n,s}(\vec{k}). \quad (2.20)$$

Here  $\vec{A}_{n,s}(\vec{k}) = i \langle u_{\vec{k},n,s} | \nabla_{\vec{k}} u_{\vec{k},n,s} \rangle = i \langle u_{\vec{k},n,s} | \nabla_{\vec{k}} | u_{\vec{k},n,s} \rangle$  is Berry connection.

We have

$$\begin{aligned}\vec{A}_{n,s}(\vec{k}) &= i \langle u_{\vec{k},n,s} | \nabla_{\vec{k}} u_{\vec{k},n,s} \rangle = \langle u_{\vec{k},n,s} | \Theta^{-1} \Theta | \nabla_{\vec{k}} u_{\vec{k},n,s} u_{\vec{k},n,s} \rangle = \langle u_{-\vec{k},n,-s} | \Theta \nabla_{\vec{k}} u_{\vec{k},n,s} \rangle \\ &= \langle u_{-\vec{k},n,-s} | \Theta \nabla_{\vec{k}} u_{\vec{k},n,s} \rangle = \langle u_{-\vec{k},n,-s} | \nabla_{-\vec{k}} u_{-\vec{k},n,s} \rangle = \vec{A}_{n,-s}(-\vec{k})\end{aligned}$$

So,

$$\Omega_{n,-s}(-\vec{k}) = \nabla_{-\vec{k}} \times \vec{A}_{n,-s}(-\vec{k}) = -\nabla_{\vec{k}} \times \vec{A}_{n,s}(\vec{k}) = -\Omega_{n,s}(\vec{k}). \quad (2.21)$$

Thus, under the time reversal symmetry not only momentum and spin change sign but also Berry curvature change sign. The result (2.15) is for spin up, so for spin down the Berry curvature must be

$$\Omega_{n,\downarrow}(\vec{k}) = n \frac{A^2 (B \cdot k^2 + M)}{2[(Bk^2 - M)^2 + A^2 \cdot k^2]^{3/2}}. \quad (2.22)$$

What about Chern number? If we look at (2.16) we can conclude quickly that Chern numbers change sign also. If (2.19) gives us the Chern number for spin up  $C_{n,\uparrow} = n$  ( $n = 1, -1$ ), we will have Chern number for spin down is  $C_{n,\downarrow} = -n$ . Later these results will help us to consider  $Z_2$  invariant of HgTe/CdTe material.

### 2.3.2 $Z_2$ invariant.

So, the time reversal symmetry requires  $C_{n,\uparrow} + C_{n,\downarrow} = 0$ . While the difference of them  $C_\sigma = (C_{n,\uparrow} - C_{n,\downarrow})/2$  defines quantized spin Hall conductivity [8]. The  $Z_2$  invariant which can help us to distinguish trivial insulators and topological insulators can be calculated as following

$$v = C_\sigma \text{ mod } 2. \quad (2.23)$$

One pointed out that  $v = 0$  stands for trivial insulators and  $v = 1$  stands for quantum



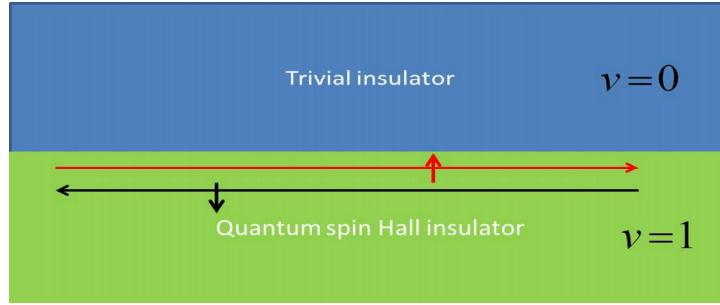


Figure 2.2: Edge states in quantum spin Hall insulator at the interface between a Quantum spin Hall insulator and an ordinary insulator.

spin Hall insulators (see Fig. 2.2). Let see in our system, what is  $\nu$ ?

For our system,  $C_\sigma = (C_{n,\uparrow} - C_{n,\downarrow}) / 2 = (1 - (-1)) / 2 = 1$  So  $\nu = 1 \bmod 2 = 1$ .  $\nu = 1$  is a nice result. It confirms that HgTe/CdTe is a 2D topological insulator (or quantum spin Hall insulator).

## 2.4 Brief summary.

The topological classification is based on the topological invariant. For trivial insulator, its  $Z_2$  invariant is equal to 0, and for non-trivial insulator is equal to 1. In this chapter we pointed out that the  $Z_2$  number of HgTe/CdTe materials is equal 1, that means HgTe/CdTe insulators are quantum spin Hall insulators. Besides, we also pointed out the change of Berry curvature and Chern number in the time reversal symmetry. The results say that under the time reversal symmetry, not only spin and momentum changed sign, but also the Berry curvature and Chern number change their sign.

# Chapter 3

## Electronic spectrum of a HgTe/CdTe quantum Hall bar.

In this chapter, we will study on the HgTe/CdTe bar system. This part will help us to understand better the Right and Left regions of the transport system. Besides, it also helps us to check our results for our model, the model that we apply electric potentials at transverse boundaries only.

### 3.1 First approach: using sine functions as basic.

We know that the sine function  $\varphi_n(y) = \sqrt{\frac{2}{W}} \sin(\frac{n\pi y}{W})$  is the solution of the Schrodinger equation for the infinite quantum well. A long y direction, the system looks like an infinite quantum well, so we can use sine functions as a basic of wave functions. Along x direction, the system has no boundaries, so the wave along x direction to be the wave function of free particle. And then we can write the wave function of system as:

$$\psi(x, y) = e^{ik_x x} \sum_n \chi_n \cdot \varphi_n(y). \quad (3.1)$$

Because the Hamiltonian (upper block) is 2x2, therefore  $\chi_n$  must be 2x1 column

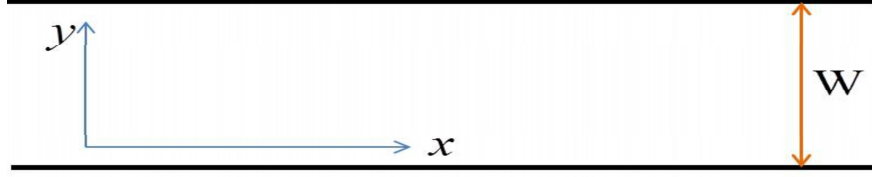


Figure 3.1: The HgTe/CdTe bar system.

matrices. In addition, they need to satisfy the normalization of wave function:

$$\langle \psi(x, y) | \psi(x, y) \rangle = \sum_{n,m} \chi_m^* \cdot \chi_n \cdot \langle \varphi_m(y) | \varphi_n(y) \rangle = \sum_{n,m} \chi_m^* \cdot \chi_n \cdot \delta_{mn} = \sum_n \chi_n^* \cdot \chi_n = 1 \quad (3.2)$$

The upper block can be written clearly:

$$\begin{aligned} H(\vec{k}) &= \begin{pmatrix} C + V - D_+ \cdot (k_x^2 + k_y^2) + M & A \cdot (k_x - ik_y) \\ A \cdot (k_x + ik_y) & C + V - D_- \cdot (k_x^2 + k_y^2) - M \end{pmatrix} \\ &= \begin{pmatrix} C + V + M - D_+ \cdot k_y^2 & -iA \cdot k_y \\ iA \cdot k_y & C + V - M - D_- \cdot k_y^2 \end{pmatrix} - k_x^2 \begin{pmatrix} D_+ & 0 \\ 0 & D_- \end{pmatrix} + k_x \begin{pmatrix} 0 & A \\ A & 0 \end{pmatrix} \end{aligned} \quad (3.3)$$

Where  $D_+ = D + B$ ,  $D_- = D - B$ .

Combining Hamiltonian and the wave function in the Schrodinger equation  $H\psi = E\psi$ , we will go to this form:

$$\left\{ \begin{aligned} &\begin{pmatrix} C + V + M - D_+ \cdot k_y^2 & -iA \cdot k_y \\ iA \cdot k_y & C + V - M - D_- \cdot k_y^2 \end{pmatrix} \sum_n \chi_n \cdot \varphi_n(y) \\ &-k_x^2 \begin{pmatrix} D_+ & 0 \\ 0 & D_- \end{pmatrix} \sum_n \chi_n \cdot \varphi_n(y) + k_x \begin{pmatrix} 0 & A \\ A & 0 \end{pmatrix} \sum_n \chi_n \cdot \varphi_n(y) \end{aligned} \right\} = E \sum_n \chi_n \cdot \varphi_n(y). \quad (3.4)$$

Let multiply both sides by  $dy \cdot \varphi_m(y)$  and taking integral along y direction, we will get

to

$$\sum_n \begin{pmatrix} (C + V + M) \delta_{mn} - D_+ \langle \varphi_m | k_y^2 | \varphi_n \rangle & -iA \langle \varphi_m | k_y | \varphi_n \rangle \\ iA \langle \varphi_m | k_y | \varphi_n \rangle & (C + V - M) \delta_{mn} - D_- \langle \varphi_m | k_y^2 | \varphi_n \rangle \end{pmatrix} \chi_n$$

$$- \sum_n k_x^2 \begin{pmatrix} D_+ & 0 \\ 0 & D_- \end{pmatrix} \delta_{mn} \chi_n + \sum_n k_x \begin{pmatrix} 0 & A \\ A & 0 \end{pmatrix} \delta_{mn} \chi_n = \sum_n E \delta_{mn} \chi_n$$

Setting:

$$\Delta_{mn}^+ = (C + V + M) \delta_{mn} - D_+ \langle \varphi_m(y) | k_y^2 | \varphi_n(y) \rangle \quad \eta_{mn} = \langle \varphi_m(y) | k_y | \varphi_n(y) \rangle$$

$$\Delta_{mn}^- = (C + V - M) \delta_{mn} - D_- \langle \varphi_m(y) | k_y^2 | \varphi_n(y) \rangle$$

$$S_{mn} = \begin{pmatrix} \Delta_{mn}^+ & -iA\eta_{mn} \\ iA\eta_{mn} & \Delta_{mn}^- \end{pmatrix}, \quad X_{mn} = \begin{pmatrix} D_+ & 0 \\ 0 & D_- \end{pmatrix} \delta_{mn}, \quad T_{mn} = \begin{pmatrix} 0 & A \\ A & 0 \end{pmatrix} \delta_{mn}.$$

Noting that  $m, n$  indices are not column and row index of matrices. For a given value of  $m, n$  we have one matrix  $S_{mn}$ , for other values we have different matrices  $S_{mn}$ .

The detail of calculation for  $\Delta_{mn}^+, \Delta_{mn}^-, \eta_{mn}$  will be shown in the appendix A. The results are

$$\Delta_{mn}^+ = (C + V + M) \delta_{mn} - D_+ \langle \varphi_m(y) | k_y^2 | \varphi_n(y) \rangle = (C + V + M) \delta_{mn} - D_+ \left( \frac{n\pi}{W} \right)^2 \delta_{mn}$$

$$\Delta_{mn}^- = (C + V - M) \delta_{mn} - D_- \langle \varphi_m(y) | k_y^2 | \varphi_n(y) \rangle = (C + V - M) \delta_{mn} - D_- \left( \frac{n\pi}{W} \right)^2 \delta_{mn}. \quad (3.5)$$

$$\eta_{mn} = \langle \varphi_m(y) | k_y | \varphi_n(y) \rangle = \begin{cases} i \frac{2mn}{(m^2 - n^2)W} [(-1)^{m+n} - 1] & \text{for } m \neq n \\ 0 & \text{for } m = n \end{cases}$$

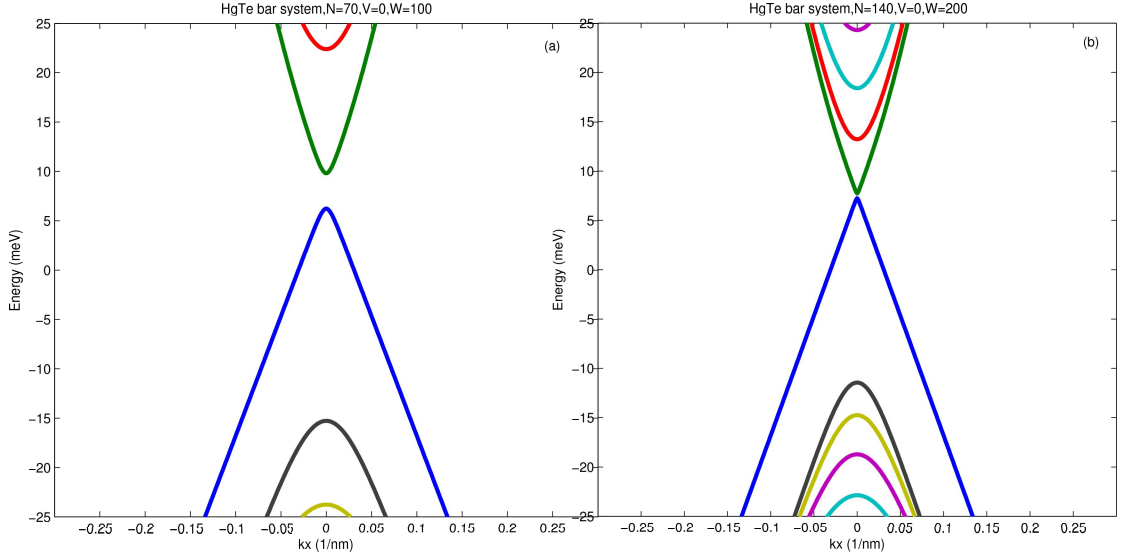


Figure 3.2: Energy dispersion of HgTe/CdTe bar system. Potential is  $V=0$  meV. The width of system is  $W=100$ nm for (a) and  $W=200$  nm for (b).

So,  $\sum_n F_{mn}\chi_n = \sum_n E\delta_{mn}\chi_n$  with  $F_{mn} = S_{mn} - k_x^2 X_{mn} + k_x T_{mn}$  If we set

$$\mathbf{F} = \begin{pmatrix} F_{11} & F_{12} & \dots & F_{1N} \\ F_{21} & F_{22} & \dots & F_{2N} \\ \cdot & \cdot & \cdot & \cdot \\ \cdot & \cdot & \cdot & \cdot \\ \cdot & \cdot & \cdot & \cdot \\ F_{N1} & F_{N2} & \dots & F_{NN} \end{pmatrix} \kappa = \begin{pmatrix} \chi_1 \\ \chi_2 \\ \cdot \\ \cdot \\ \cdot \\ \chi_N \end{pmatrix} \quad (3.6)$$

We will stay at the Eigen problem

$$\mathbf{F}\kappa = E.\kappa. \quad (3.7)$$

This form is very nice for numerical programs.

In the Fig. 3.2, we have energy dispersions for HgTe/CdTe bar system. Because of the finite size effect, the energy bands open an edge gap and this gap is falling within the bulk gap. When the width of system is smaller, then the edge gap opens bigger and

CHAPTER 3. ELECTRONIC SPECTRUM OF A HGTE/CDTE QUANTUM HALL BAR.

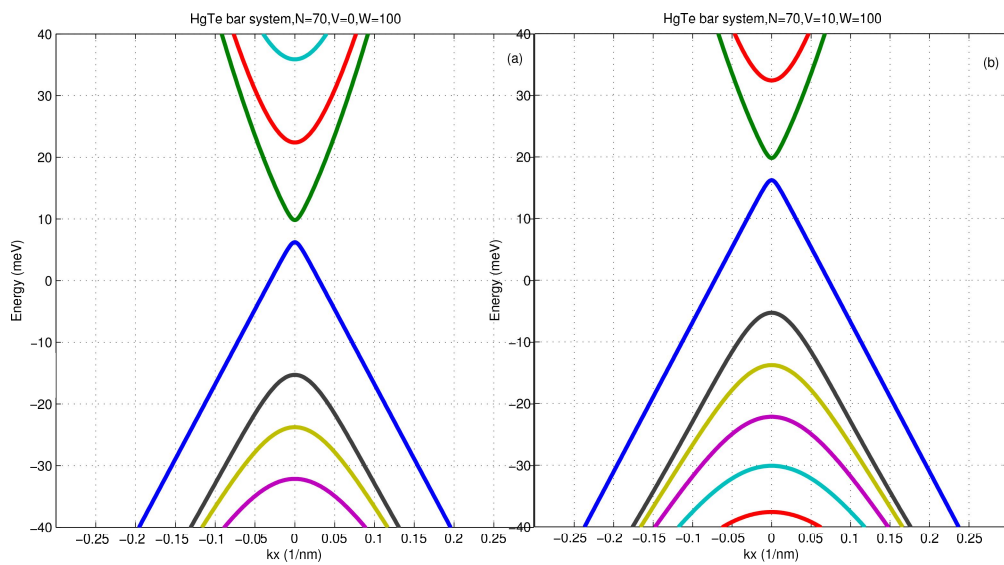


Figure 3.3: Energy dispersion of HgTe/CdTe bar system. The width of system is  $W=100\text{nm}$ . Potential is  $V=0\text{ meV}$  for (a) and  $V=10\text{ meV}$  for (b).

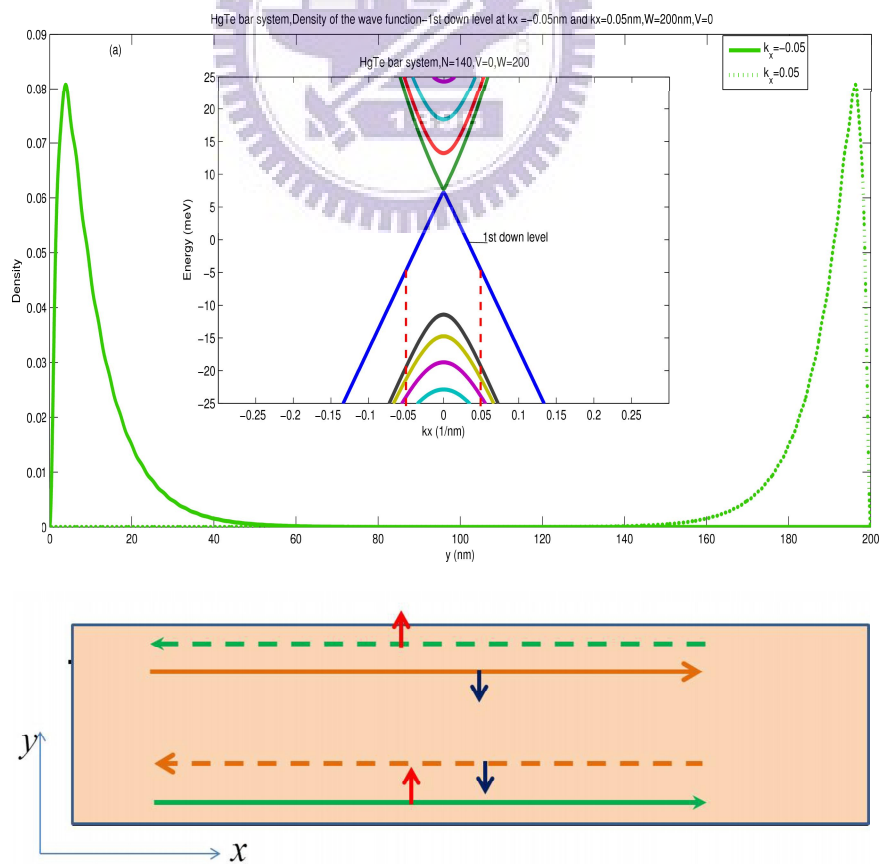


Figure 3.4: (a) Density of edge states at  $k=0.05$  and  $k=-0.05\text{ nm}$ . Other parameters are  $W=200\text{ nm}$ ,  $V=0\text{ meV}$ . (b) Edge states at each boundary.

vice versa. (See the Fig. 3.2 (a),  $W = 100$ , the edge gap is bigger than the Fig. 3.2 b's.). Since we fix parameters and only change the value of potential, the result is shown in the Fig. 3.3. The result shows that the whole energy dispersion is shifted up or down since we change potential. Nothing else changed in the energy dispersion. So, essentially the potential in this system does not deform physics of the system if we just examine the energy dispersion or wave functions. It means that physics are not changed if we only consider  $V = 0$  case. However, potential is reason of scattering, so in the transport system we need to consider potential also. In the Fig. 3.4 are density of edge states and the sketch of edge states locate in the HgTe/CdTe bar system. The values of parameters of system are  $W=200$  nm,  $V = 0$  meV . The edge states are considered at the points  $k_x = -0.05$  nm and  $k_x = 0.05$  nm which are shown in the picture of the energy dispersion. Density of edge state at  $k_x = -0.05$  nm says that it is located nearly the bottom edge (nearby  $y = 0$ ), and from the energy dispersion we can see that group velocity of this edge state is positive, that means the wave is right-moving wave. In the system in figure (b), this edge state is indicated by the green solid line with the direction is towards right. We have the red arrow upwards is indicated for spin up of electrons. At the point  $k_x = 0.05$ , we have another edge state which was plotted by the green dot line. Unlike the former edge state, this edge state locates nearly the top edge (nearby  $y = W$ ). And from the energy dispersion, we know the direction of the group velocity for this state is left-moving. Because of these things, in the figure (b), the second edge state is described by a green dot line towards the left. Of course, the second edge state has the same spin up with the first edge state due to they come from the same block of Hamiltonian.

But we do not have only these two edge states, but also have two other edge states because of time reversal symmetry. The other edge states come from the lower block of Hamiltonian for spin down. We know that, under the action of time reversal operator, both momentum and spin change sign. So, the edge state which is indicated by the green solid line in the Fig. (b) will have a "brother" with spin down and the direction of moving is towards the left, it is opposite direction with the green solid wave. The edge state with

spin down is described by the orange dot line in the Fig. (b). Thus, the green solid edge state and the orange dot edge state are a couple due to the time reversal symmetry. Similar, the spin up-green dot line is also in another couple and its partner is an edge state with spin down and the direction of moving is towards the right. This state is described by the orange solid line in the Fig. (b).

### 3.2 Second approach: using exponent functions as trial functions.

In this approach, we can focus more deeply on the edge states. This is a very nice way for seeking physics of edge states nearby gamma point. Not only that, we also can get some analytical results for the limited case with the width  $W$  closes to infinite. And we have semi-infinite system. In physics, if analytical result is possible, it is better than numerical result. This is the reason that similar calculations were published on Physical Review Letter [4]. We will try with a trial function as

$$\psi(x, y) = e^{ik_x x} \chi e^{\lambda y} \quad (3.8)$$

Applying to the Schrodinger equation we have:

$$\begin{pmatrix} C + V - D_+.(k_x^2 + k_y^2) + M & A.(k_x - ik_y) \\ A.(k_x + ik_y) & C + V - D_-.(k_x^2 + k_y^2) - M \end{pmatrix} e^{ik_x x} \chi e^{\lambda y} = E e^{ik_x x} \chi e^{\lambda y} \quad (3.9)$$

Let see  $k_x, k_y$  as operators and they act on the exponential functions. After that we can cancel  $e^{ik_x x}, e^{\lambda y}$  on both sides without any mistake.

$$\begin{pmatrix} C + V - D_+.(k_x^2 - \lambda^2) + M - E & A.(k_x - \lambda) \\ A.(k_x + \lambda) & C + V - D_-.(k_x^2 - \lambda^2) - M - E \end{pmatrix} \chi = 0 \quad (3.10)$$



And then we get

$$\det \begin{pmatrix} \alpha_+ - D_+ \cdot (k_x^2 - \lambda^2) & A \cdot (k_x - \lambda) \\ A \cdot (k_x + \lambda) & \alpha_- - D_- \cdot (k_x^2 - \lambda^2) \end{pmatrix} = 0$$

Here

$$\alpha_+ = C + V + M - E, \alpha_- = C + V - M - E. \quad (3.11)$$

This equation allows us examine  $\lambda$  in the values of E. We have 4 solutions  $\pm\lambda_1, \pm\lambda_2$  from this equation with

$$\lambda_1 = \sqrt{k_x^2 - F + \sqrt{F^2 - \frac{\alpha_+ \alpha_-}{D_+ D_-}}}, \lambda_2 = \sqrt{k_x^2 - F - \sqrt{F^2 - \frac{\alpha_+ \alpha_-}{D_+ D_-}}}, \quad (3.12)$$

where

$$F = \frac{A^2 + D_+ \alpha_- + D_- \alpha_+}{2 \cdot D_+ D_-}.$$

So, the wave function must be the superposition of these solutions, given as follows

$$\Phi(x, y) = e^{ik_x x} \left[ \alpha \begin{pmatrix} a_1 \\ b_1 \end{pmatrix} e^{\lambda_1 y} + \alpha' \begin{pmatrix} a_1' \\ b_1' \end{pmatrix} e^{-\lambda_1 y} + \beta \begin{pmatrix} a_2 \\ b_2 \end{pmatrix} e^{\lambda_2 y} + \beta' \begin{pmatrix} a_2' \\ b_2' \end{pmatrix} e^{-\lambda_2 y} \right]. \quad (3.13)$$

We need to determine the superposition coefficients  $\alpha, \alpha', \beta, \beta'$ . The relation between a's and b's, which are the coefficients for a normalized pseudospin, can be found directly from the Schrodinger equation, given also in Eq. (3.10)

$$\begin{pmatrix} C + V - D_+ (k_x^2 - \lambda^2) + M - E & A (k_x - \lambda) \\ A (k_x + \lambda) & C + V - D_- (k_x^2 - \lambda^2) - M - E \end{pmatrix} \begin{pmatrix} a \\ b \end{pmatrix} = 0,$$

to give

$$\begin{aligned} b &= \frac{-A(k_x + \lambda)a}{C + V - D_- (k_x^2 - \lambda^2) - M - E} \\ &= \frac{-A k_x a}{C + V - D_- (k_x^2 - \lambda^2) - M - E} + \frac{-A \lambda a}{C + V - D_- (k_x^2 - \lambda^2) - M - E} = a.X + aY. \end{aligned}$$

$$\text{Here } X = \frac{-A k_x}{C + V - D_- (k_x^2 - \lambda^2) - M - E}, \quad Y = \frac{-A \lambda}{C + V - D_- (k_x^2 - \lambda^2) - M - E}.$$

E.q (3.13) then becomes

$$\Phi(x, y) = e^{ik_x x} \begin{bmatrix} \alpha_1 \begin{pmatrix} 1 \\ X_1 + Y_1 \end{pmatrix} e^{\lambda_1 y} + \alpha_1' \begin{pmatrix} 1 \\ X_1 - Y_1 \end{pmatrix} e^{-\lambda_1 y} \\ + \beta_1 \begin{pmatrix} 1 \\ X_2 + Y_2 \end{pmatrix} e^{\lambda_2 y} + \beta_1' \begin{pmatrix} 1 \\ X_2 - Y_2 \end{pmatrix} e^{-\lambda_2 y} \end{bmatrix}. \quad (3.14)$$

In the final form of the wave function, we already combined notations  $a$  and  $\alpha, \beta$  in new notations are  $\alpha_1, \beta_1$ .

Now we will go to the important point which helps us to look for edge states. Applying this wave function for the vanishing condition of the wave function at the two boundaries  $y = 0$  and  $y = W$  we will get 2 matrix equations. In fact we have 4 equations because each matrix equation from the boundary conditions gives us 2 equations. Therefore we have enough equations to solve 4 parameters  $\alpha_1, \alpha_1', \beta_1, \beta_1'$ . Because of the unique property of solution, it leads to an important relation that we can look for edge states from this

relation.

$$\det \begin{vmatrix} e^{\lambda_1 W/2} & e^{-\lambda_1 W/2} & e^{\lambda_2 W/2} & e^{-\lambda_2 W/2} \\ (X_1 + Y_1) e^{\lambda_1 W/2} & (X_1 - Y_1) e^{-\lambda_1 W/2} & (X_2 + Y_2) e^{\lambda_2 W/2} & (X_2 - Y_2) e^{-\lambda_2 W/2} \\ e^{-\lambda_1 W/2} & e^{\lambda_1 W/2} & e^{-\lambda_2 W/2} & e^{\lambda_2 W/2} \\ (X_1 + Y_1) e^{-\lambda_1 W/2} & (X_1 - Y_1) e^{\lambda_1 W/2} & (X_2 + Y_2) e^{-\lambda_2 W/2} & (X_2 - Y_2) e^{\lambda_2 W/2} \end{vmatrix} = 0. \quad (3.15)$$

The calculation for this relation can make you feel bored. But if we do work, we have no other choice. We want to show immediately the result of the calculation as following

$$\frac{1 - \cosh(\lambda_1 W) \cosh(\lambda_2 W)}{\sinh(\lambda_1 W) \sinh(\lambda_2 W)} = \frac{(X_2 - X_1)^2 - Y_2^2 - Y_1^2}{2Y_2 Y_1}. \quad (3.16)$$

The left hand side of Eq. (3.16) is rewritten as  $-\frac{1}{2} \left[ \frac{\tanh(\lambda_1 W/2)}{\tanh(\lambda_2 W/2)} + \frac{\tanh(\lambda_2 W/2)}{\tanh(\lambda_1 W/2)} \right]$ . After some more steps of calculation. Besides, the right also can be written in a better form with using a new notation

$$L = C + V - D_-. (k_x^2 - \lambda^2) - M - E. \quad (3.17)$$

Combining all things together and then we have

$$\frac{\tanh(\lambda_1 W/2)}{\tanh(\lambda_2 W/2)} + \frac{\tanh(\lambda_2 W/2)}{\tanh(\lambda_1 W/2)} = \frac{L_2^2 \lambda_1^2 + L_1^2 \lambda_2^2 - k_x^2 (L_2 - L_1)^2}{L_1 L_2 \lambda_1 \lambda_2}. \quad (3.18)$$

One more time, we want to emphasize that the calculations from E.q (3.15) to E.q (3.16) and E.q (3.16) to E.q (3.18) are quite hard and long. But with the aim is physical meaning of results so some steps will be said in key words that would be not in details.

Because  $\lambda, L$  are functions of energy which are given by (3.12) and (3.17). So with a given width  $W$ , since we give a value of  $k_x$  in to E.q (3.18) we will get the solution of  $E$ . It means we can get relation between  $E$  and  $k_x$  via E.q (3.18) by numerical method. Because

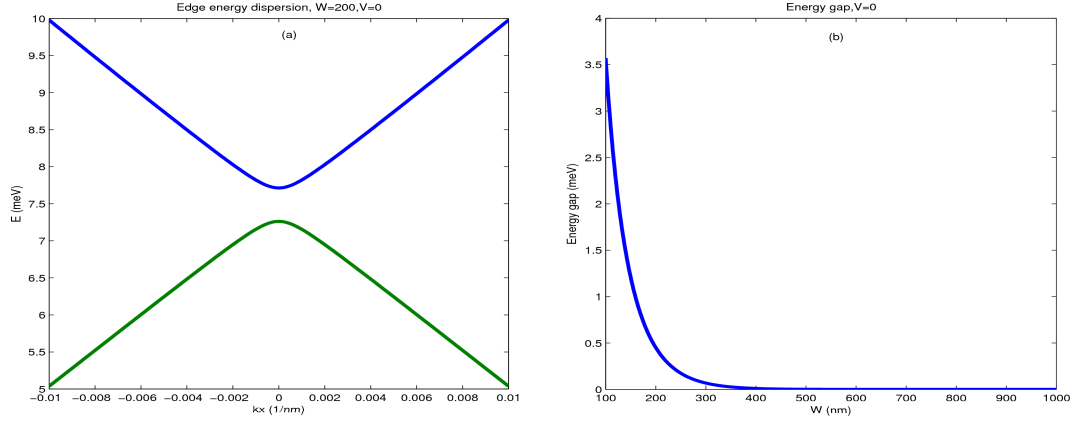


Figure 3.5: (a) Edge energy dispersion at  $W=200\text{nm}$  and  $V=0$  meV. (b) The dependence of energy gap on the width of system.

the Eq. (3.18) is obtained from the condition of wave function at the two boundaries. So this relation between  $E - k_x$  reflects the structure of energy of edge states.

The numerical result in the Fig. 3.5 (a) shows that we have a gap in the energy dispersion of edge states. And edge states look perfectly linear around the gamma point. Besides, the Fig. 3.5 (b) tells us the dependence of edge gap on the width of system. Since the width is increased, the gap becomes smaller. This result is completely reasonable with the finite size effect. In the Fig. (b), we can see that the edge gap decays exponentially. At the width is 500 nm, the gap almost closes to zero. But the gap never equals to zero because of the finite size effect, even it can be very small. The two edge curves will be crossing and we have gapless in the case of semi-infinite system. We can get the result for this particular case by taking limit of the result of the equation (3.18) since  $W$  closes to infinite. The work is not easy, but we will be happy because we can get analytical results which are always expectation of physicists.

Since  $W$  closes to infinite,  $\lim \tanh(\lambda W/2) \rightarrow 1$ , thus the left hand side of Eq. (3.18) would be  $1+1=2$ . And then the Eq. (3.18) becomes  $k_x^2(L_2 - L_1)^2 = (L_2\lambda_1 - L_1\lambda_2)^2$ . Now we use the relations (3.17) of  $L$ , (2.11) of  $\alpha_+, \alpha_-$  and (3.12) of  $\lambda, F$  and turns inserting into the result which we have just gotten, we will get a nice form for edge states

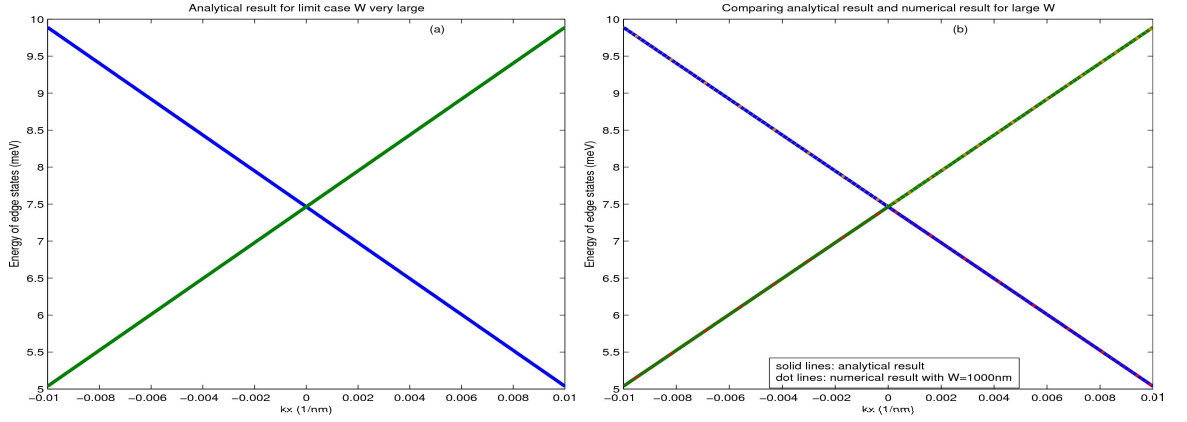


Figure 3.6: (a) plotting of analytical result for the limited case semi-infinite. (b) Comparison of analytical result for limit case and numerical result for the case of the width is large enough.

as following

$$E = C + V - \frac{MD}{B} \pm \frac{A}{B} \sqrt{-D_+ D_-} k_x. \quad (3.19)$$

So, this method can provide us a good result for the limited case of the width- the case of semi-infinite. The edge states for a semi-infinite system are completely linear on momentum. The two linear lines correspond to two different directions of moving. They are opposite direction. This analytical result can be checked by the result from the Fig. 3.5(b). From the Fig. 3.5(b) we can see that at  $W = 1000nm$ , the edge gap very small and nearby 0. That means the numerical result for  $W = 1000nm$  and the analytical results for the semi-infinite are almost coincided.

The result of Fig. 3.6 (b) confirms the correctness of the analytical result for the semi-infinite case.

### 3.3 Comparing results of two approaches.

We can compare two approaches in the results of edge states.

In the Fig. 3.7 we can see that both approaches give us the same edge states. This is

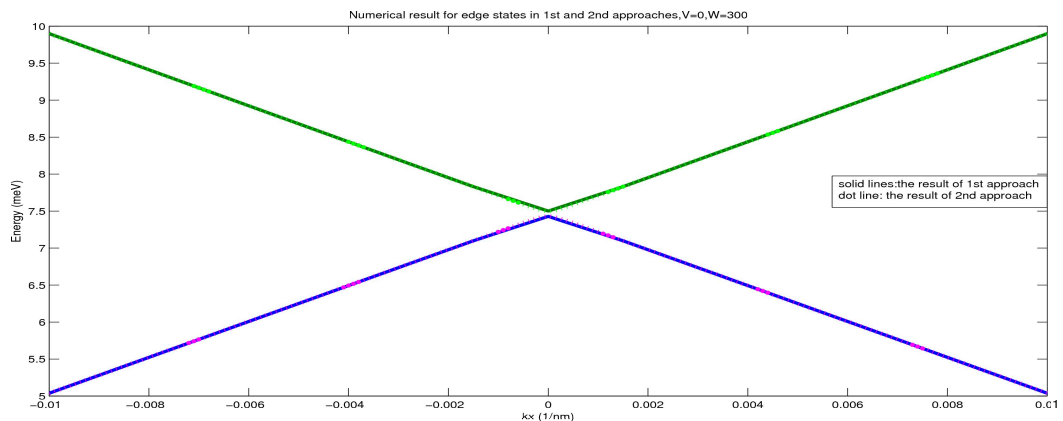


Figure 3.7: Comparing the result of edge states in the two approaches. The parameters are  $W=300$ ,  $V=0$ .

a nice result.

### 3.4 Brief summary.

The results that we got in this chapter are the energy structure and wave functions of HgTe/CdTe bar. The most interest here is the construction of edge states. Results point out that we have 2 pairs of edge states. For spin up, we have 2 edge states locate at different sides of the system and their moving directions are opposite. Similar, we have the two other edge states for spin down. Besides, the method using the exponential functions as trial functions also provide us analytical result for the case of semi-infinite. The comparison of the edge states in the two approaches indicates that the results for edge states are exactly the same.

# Chapter 4

## Electronic band of a split gated HgTe/CdTe quantum Hall bar

In chapter 3 we saw that when potentials were applied in the HgTe/CdTe bar in the way that the potential be filled the whole system, the energy dispersion just shifts up or down without any change. Because edge states are particular feature of topological insulators, so in this chapter we will study more physics by controlling edge states via potentials applied at transverse boundaries of the HgTe/CdTe bar system.

### 4.1 The equation to determine energy dispersion of the new system.

Doing in the similar way in the chapter 3, we use the approach with sine functions. From the Schrodinger equation, we can reduce to the equation

$$\sum_n (S_{mn} - k_x^2 X_{mn} + k_x T_{mn}) \chi_n = 0 \quad (4.1)$$

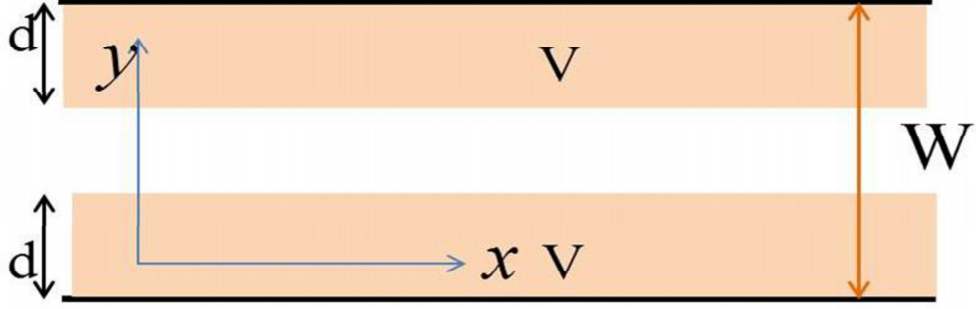


Figure 4.1: The two split gates system with electric potentials are applied at transverse boundaries.

Where

$$S_{mn} = \begin{pmatrix} \Delta_{mn}^+ & -iA\eta_{mn} \\ iA\eta_{mn} & \Delta_{mn}^- \end{pmatrix}, X_{mn} = \begin{pmatrix} D_+ & 0 \\ 0 & D_- \end{pmatrix} \delta_{mn}, T_{mn} = \begin{pmatrix} 0 & A \\ A & 0 \end{pmatrix} \delta_{mn} \quad (4.2)$$

$$\Delta_{mn}^+ = (C + M) \delta_{mn} + \langle \varphi_m(y) | V(y) | \varphi_n(y) \rangle - D_+ \langle \varphi_m(y) | k_y^2 | \varphi_n(y) \rangle \quad (4.3)$$

$$\Delta_{mn}^- = (C - M) \delta_{mn} + \langle \varphi_m(y) | V(y) | \varphi_n(y) \rangle - D_- \langle \varphi_m(y) | k_y^2 | \varphi_n(y) \rangle$$

$$\eta_{mn} = \langle \varphi_m(y) | k_y | \varphi_n(y) \rangle.$$

But in this model, something is different. We just integrate from  $0 \leq y \leq d$  and  $(W - d) \leq y \leq W$  on  $V(y)$ . And thus, the results are

+ For  $m \neq n$

$$\eta_{mn} = \langle \varphi_m(y) | k_y | \varphi_n(y) \rangle = i \frac{2mn}{(m^2 - n^2)W} [(-1)^{m+n} - 1]$$

$$\Delta_{mn}^+ = \frac{V}{W} \left\{ \frac{W}{(m-n)\pi} \sin\left(\frac{m-n}{W}\pi d\right) - \frac{W}{(m+n)\pi} \sin\left(\frac{m+n}{W}\pi d\right) \right\} \cdot [1 + (-1)^{m+n}] + (C + M) \delta_{mn} - D_+ \left(\frac{n\pi}{W}\right)^2 \delta_{mn} \quad (4.4)$$

$$\Delta_{mn}^- = \frac{V}{W} \left\{ \frac{W}{(m-n)\pi} \sin\left(\frac{m-n}{W}\pi d\right) - \frac{W}{(m+n)\pi} \sin\left(\frac{m+n}{W}\pi d\right) \right\} \cdot [1 + (-1)^{m+n}] + (C - M) \delta_{mn} - D_- \left(\frac{n\pi}{W}\right)^2 \delta_{mn}$$



+ For  $m = n$

$$\eta_{mn} = \langle \varphi_n(y) | k_y | \varphi_n(y) \rangle = 0$$

$$\Delta_{mn}^+ = (C + M) + \frac{2V}{W} \left\{ d - \frac{W}{2m \cdot \pi} \sin\left(\frac{2m}{W} \pi d\right) \right\} - D_+ \left(\frac{n\pi}{W}\right)^2 \cdot \delta_{mn} \quad (4.5)$$

$$\Delta_{mn}^- = (C - M) \delta_{mn} + \frac{2V}{W} \left\{ d - \frac{W}{2m \cdot \pi} \sin\left(\frac{2m}{W} \pi d\right) \right\} - D_- \left(\frac{n\pi}{W}\right)^2 \cdot \delta_{mn}$$

Now we target to the Eigen problem by set up some things. We set  $F_{mn} = S_{mn} - k_x^2 X_{mn} + k_x T_{mn}$  So,  $\sum_n F_{mn} \chi_n = \sum_n E \cdot \delta_{mn} \chi_n$ . If we set

$$\mathbf{F} = \begin{pmatrix} F_{11} & F_{12} & \dots & F_{1N} \\ F_{21} & F_{22} & \dots & F_{2N} \\ \cdot & \cdot & \cdot & \cdot \\ \cdot & \cdot & \cdot & \cdot \\ \cdot & \cdot & \cdot & \cdot \\ F_{N1} & F_{N2} & \dots & F_{NN} \end{pmatrix} \kappa = \begin{pmatrix} \chi_1 \\ \chi_2 \\ \cdot \\ \cdot \\ \cdot \\ \chi_N \end{pmatrix} \quad (4.6)$$

We will go to the Eigen problem:

$$\mathbf{F} \kappa = E \cdot \kappa. \quad (4.7)$$

Making programs to run this equation, we will get the energy dispersion. Let see results in the next part.

## 4.2 Result of energy dispersion.

Before we go to the numerical results of this system, we can guess some things on this system as following: (1) It is not the same the system in chapter 3, in this system something changes in the energy dispersion. Because the potentials are applied at transverse

boundaries only, so edge states will be affected by potentials much more than bulk states. (2) Edge states will be not moved out of the potential areas, they still locate nearly edges even some thing changes. Because, if edge states were moved out of the potential areas then when  $d$  closes to  $W/2$ , the edge states would locate at the middle of the system. This is funny thing. So, edge states must locate nearly edges still. (3) Since  $d = 0$  and  $d = W/2$ , the results of this system must be identical to the results of the system in chapter 2.

#### 4.2.1 Special cases: $d = 0$ and $d = W/2$ .

First we can check results of the new system by special cases. We know that if  $d = 0$ , that means we have no potentials areas in the system and thus the system becomes the system which is HgTe/CdTe bar with  $V = 0$  we considered in the chapter 3. Not only that, we also can check for the case  $d = W/2$ . In this case we go the the case that the electric potential fills the whole system. And we can compare with the result of the system in chapter 3 for  $V \neq 0$ .

Look at the results of the Fig. 6.2, we see that the results of two system are exactly the same. This helps us to believe that we are in the correct direction to consider the new system.

#### 4.2.2 Result for other cases.

What we expect in the new system is the effect of potentials to the energy dispersion. This effect is interesting since  $0 < d < W/2$ . Now the system is in a different physics due to the potentials just affect to a part of the system. The Fig. 4.3 shows us new energy dispersion, and then we can see the difference with the former results.

From the Fig. 4.3 we can see that the effect of the potentials on the edge states is stronger than on the the bulk states. This is reasonable because the potentials only applied nearly transverse boundaries. In addition, we also see that in the bulk bands, for

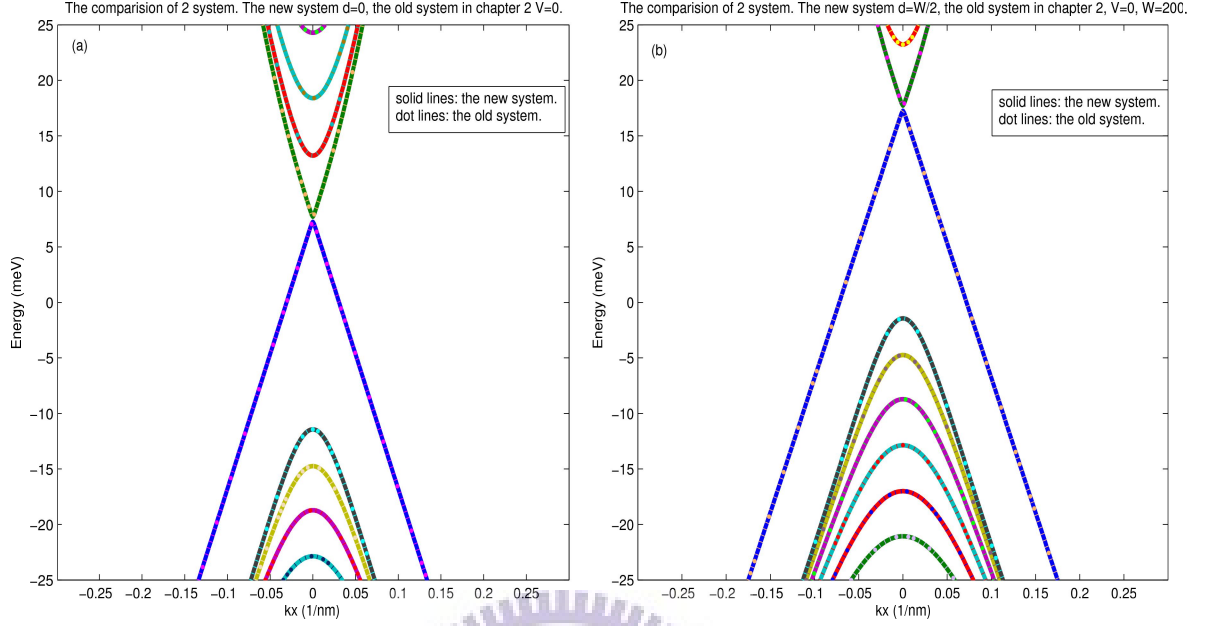


Figure 4.2: Comparison of energy dispersion of the system in chapter 3 and the new system (a)  $d=0$  for the new system and  $V=0$  for the old system. (b)  $d=W/2$ ,  $V=10$  for the new system and  $V=10$  for the old system. Here  $W=200\text{nm}$ .

sub bands which have higher index will be affected stronger than lower index sub band. Here the band index is conventional from the top band of lower bands and the bottom band of the upper bands. This result can be explained by the Fig. 4.4. In the Fig. 4.4 we plot density of down bands at  $k_x = 0$ . The picture shows that edge states are the nearest the edges and the 2nd down band (1st bulk down band) is the farthest the edges. Therefore, the effect of potentials is the strongest on the edge states and the weakest on the 1st bulk band. For other bulk bands from 2nd index, the effect of potentials is increasing gradually.

### 4.3 Edge states in the system.

The interests in this system are the change of edge states under the effect of the potentials. Look at the Fig. 4.4 we can see that this change is completely different from the different of the system in chapter 3. Almost states are changed under the effect of

## CHAPTER 4. ELECTRONIC BAND OF A SPLIT GATED HGTE/CDTE QUANTUM HALL BAR

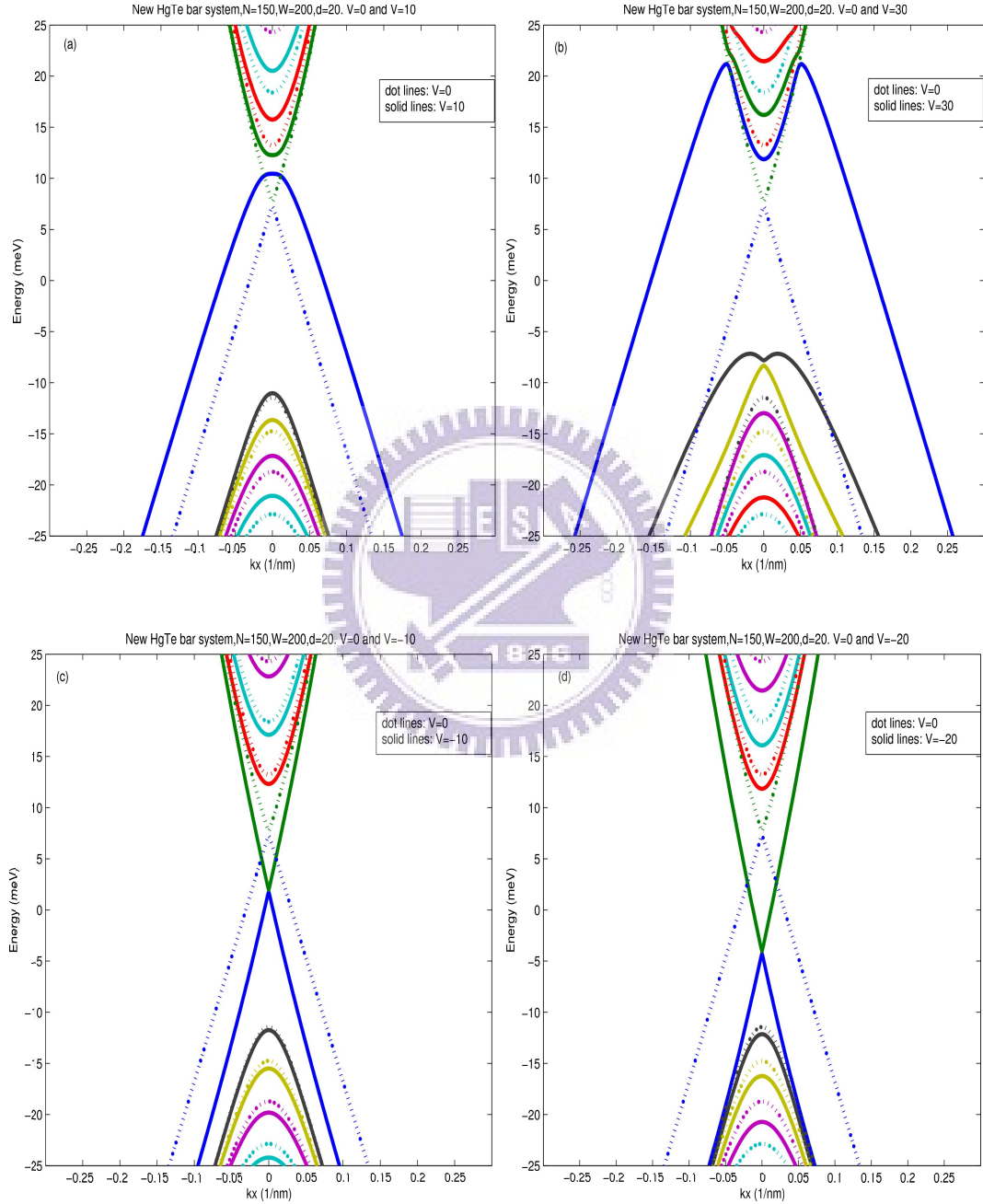


Figure 4.3: The difference in the energy dispersion when we change potentials. (a)  $V=10\text{meV}$ . (b)  $V=30\text{meV}$ . (c)  $V=-10\text{meV}$ . (d)  $V=-20\text{meV}$ . Here  $W=200\text{nm}$ .

CHAPTER 4. ELECTRONIC BAND OF A SPLIT GATED HGTE/CDTE QUANTUM HALL BAR

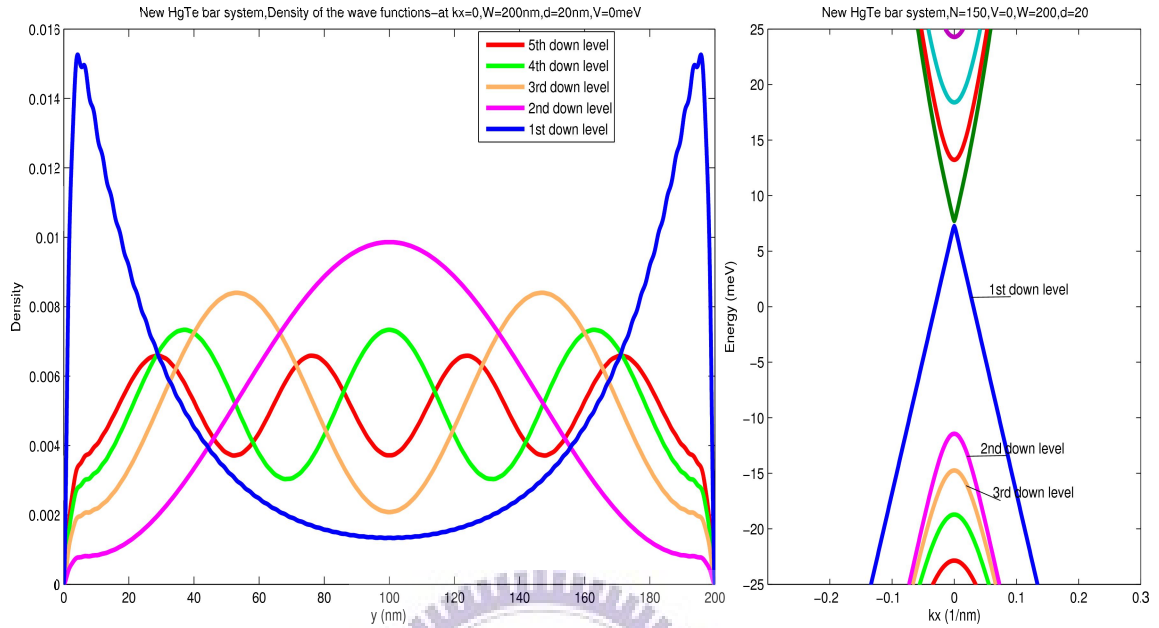


Figure 4.4: Density of wave functions for down bands, with the case  $V=0$ . Here  $W=200\text{nm}$ .

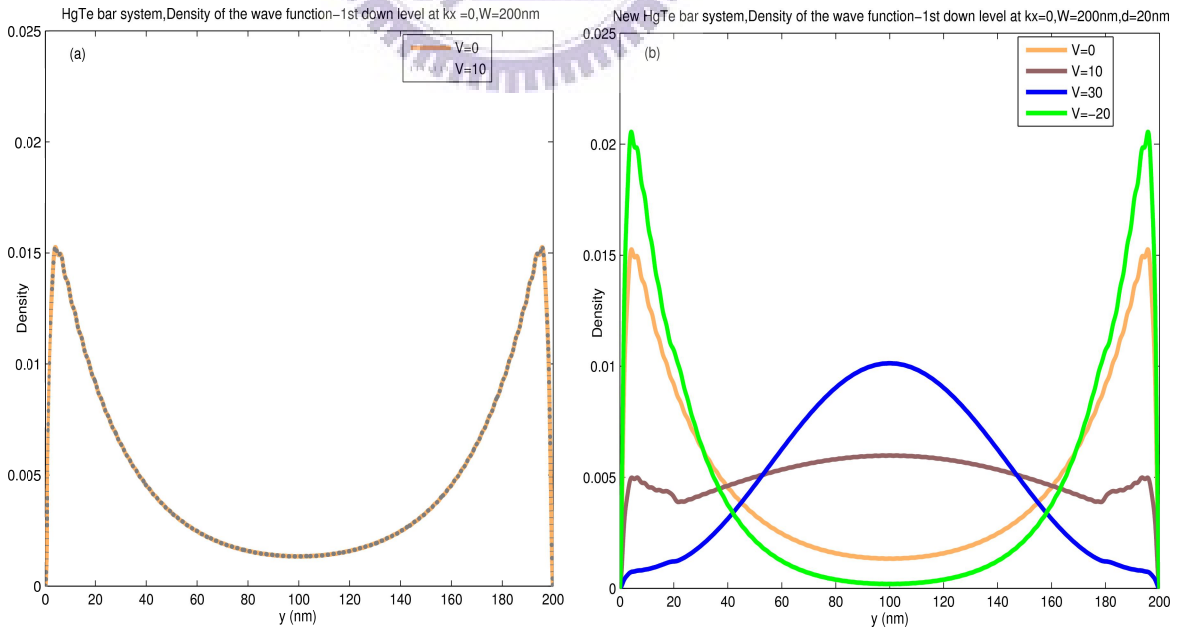


Figure 4.5: (a) edge states (1st down level) at  $k_x = 0$  under the change of potential. The consideration is in the HgTe/CdTe bar system in chapter 3. (b) Edge states (1st down level) at  $k_x = 0$  under the change of potentials. The consideration is in the new HgTe/CdTe bar system

potentials, especially edge states. The Fig. 4.4 (a) shows that since we change potentials, the edge gap can be changed. For  $V = 10meV$ , the edge gap become bigger. This means we can control the gap of edge states by suitable potentials. Besides, the Fig. 4.4 (b) gives us another new physics. At the point  $k_x = 0$  of the 1st down band, it does not look like edge state any more. This is correct. For the Fig. 4.4 (b) with  $V = 30meV$ , we have the corresponding density of edge state in the Fig. 4.5 (b), it is the blue curve. Clearly that the blue curve is like bulk state, it is not like edge state any more. So, with a strong enough potential, we can destroy edge states around the gamma point. We can explain the destroying as follow: because edge states are affected much more than bulk states, so they are moved longer than bulk states. If the potentials are large enough, the edge states will be moved very nearly bulk states and thus a strong mixing of edge state and bulk states is constructed. It makes edge states now having behavior of bulk states. On the Fig. 4.4 (c) and (d) we can see some other change of edge state under the change of potentials. In both cases, we use negative potentials. So we can "pull" edge states down. The Fig. 4.5 (a) shows the density of the edge state (1st down level) at  $k_x = 0$  for two values of potentials in the HgTe/CdTe bar in chapter 3. Nothing changes in this figure. It means potentials do not change physics of edge states in that system. But the story is completely different in the new system. The Fig. 4.5 (b) shows that when we change potentials, the behavior of edge states can be changed. At  $V = 0$  we have the same result as the figure (a). But when  $V = 10meV$  (brown curve), due to the wave of edge state overlap the wave of bulk states so the brown curve looks strange. For  $V = -20meV$ , we have the green curve. Because we use a negative potential, so it "pulls" edge state far from the bulk states of upper bands. It is reason why edge states become nicer.

#### 4.4 Brief summary.

In this chapter we have studied the effect of the two split gates system on the states, especially on the edge states and we got some new results on this system. The new

results here are that the energy shifts for the bulk-like subbands are different from the edge-like subbands under effect of the gate potentials. Specifically, edge-like subbands are affected much more than the bulk-like subbands in their energy spectrum. On the other hand, based on the wave function profiles, we find out that the edge states survive under the effects of the split gate potentials. Even though the  $k_x \approx 0$  edge state could be destroyed, finite  $k_x$  edge-states survive. Whenever the edge states exist, their spatial profiles are always in the vicinity of the quantum spin Hall bar boundaries, and not in the neighborhood of the gate boundaries. We also see that, under the influence of the potentials of the electric gates, the edge gap opening can be varied and goes to zero in the large gate potential magnitude regime. Thus, thanks to the electric gates, we can control edge states in the system.



## Chapter 5

# Quantum transport in HgTe/CdTe quantum point contact.

In this chapter we will study transport properties in HgTe/CdTe topological insulator materials. The quantum transport system is made from the system in chapter 3 and the system in chapter 4. The left region and right region we do not apply potentials, they are exactly the system which we considered in chapter 3. The middle region is made from the system in chapter 4, which with 2 potentials applied at transverse boundaries. So, our quantum transport system looks like a quantum point contact. In the transport problems, we need to know clearly wave functions in each region. Before we combine eigenstates of the Schrodinger equation in a superposition, we will find the eigenstate in the form

$$\psi(x, y) = e^{ik_x x} \sum_n \chi_n \cdot \varphi_n(y). \quad (5.1)$$

With  $\varphi_n(y) = \sqrt{\frac{2}{W}} \sin(\frac{n\pi y}{W})$ . Unlike the problem of finding energy dispersion, in this problem for a given incident energy E we need to find out  $k_x$  and  $\chi_n$  and plug them into the general form of wave function to know specifically the wave function. So, we can not use equation which is similar equation (3.7) or (4.7) to find eigenstates. We need to make a new equation which can allow us finding  $k_x$  and  $\chi_n$  from a give E.



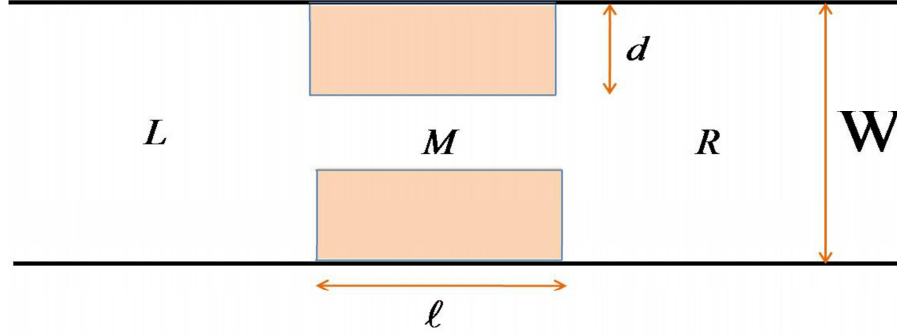


Figure 5.1: The quantum transport model based on the HgTe/CdTe topological insulator material.

## 5.1 The equation to determine $k_x$ and $\chi_n$ .

We also start from the Schrodinger equation to get the numerical formula for the transport problem. Inserting the form of wave function (5.1) in to the Schrodinger equation  $H\psi = E\psi$  we will get to the result

$$\left\{ \begin{array}{l} \left( \begin{array}{cc} C + V(y) + M - D_+ \cdot k_y^2 - E & -iA \cdot k_y \\ iA \cdot k_y & C + V(y) - M - D_- \cdot k_y^2 - E \end{array} \right) \sum_n \chi_n \cdot \varphi_n(y) \\ -k_x^2 \left( \begin{array}{cc} D_+ & 0 \\ 0 & D_- \end{array} \right) \sum_n \chi_n \cdot \varphi_n(y) + k_x \left( \begin{array}{cc} 0 & A \\ A & 0 \end{array} \right) \sum_n \chi_n \cdot \varphi_n(y) \end{array} \right\} = 0. \quad (5.2)$$

Now notice that  $V(y)$  varies in a particular way,  $0 \leq y \leq d, V(y) = V; d \leq y \leq (W - d) : V(y) = 0$  and  $(W - d) \leq y \leq W : V(y) = V$ . So when we multiply  $\int dy \cdot \varphi_m(y)$  by both sides of equation (5.2) and calculate integral, we need to give an attention carefully on the integral of  $V(y)$ . The result after the calculation is

$$\sum_n \left( \begin{array}{cc} \Delta_{mn}^+ & -iA\eta_{mn} \\ iA\eta_{mn} & \Delta_{mn}^- \end{array} \right) \chi_n - \sum_n k_x^2 \left( \begin{array}{cc} D_+ & 0 \\ 0 & D_- \end{array} \right) \delta_{mn} \chi_n + \sum_n k_x \left( \begin{array}{cc} 0 & A \\ A & 0 \end{array} \right) \delta_{mn} \chi_n = 0.$$

Here

$$\begin{aligned}\Delta_{mn}^+ &= (C + M - E) \delta_{mn} + \langle \varphi_m(y) | V(y) | \varphi_n(y) \rangle - D_+ \langle \varphi_m(y) | k_y^2 | \varphi_n(y) \rangle . \\ \Delta_{mn}^- &= (C - M - E) \delta_{mn} + \langle \varphi_m(y) | V(y) | \varphi_n(y) \rangle - D_- \langle \varphi_m(y) | k_y^2 | \varphi_n(y) \rangle . \\ \eta_{mn} &= \langle \varphi_m(y) | k_y | \varphi_n(y) \rangle .\end{aligned}\quad (5.3)$$

If we calculate in detail, we have

+ For  $m \neq n$

$$\begin{aligned}\eta_{mn} &= \langle \varphi_m(y) | k_y | \varphi_n(y) \rangle = 0. \\ \Delta_{mn}^+ &= (C + M - E) + \frac{2V}{W} \left\{ d - \frac{W}{2m\pi} \sin\left(\frac{2m}{W}\pi d\right) \right\} - D_+ \left(\frac{n\pi}{W}\right)^2 \delta_{mn} \\ \Delta_{mn}^- &= (C - M - E) \delta_{mn} + \frac{2V}{W} \left\{ d - \frac{W}{2m\pi} \sin\left(\frac{2m}{W}\pi d\right) \right\} - D_- \left(\frac{n\pi}{W}\right)^2 \delta_{mn}\end{aligned}\quad (5.4)$$

So, the matrix equation can be written as

$$\sum_n \begin{pmatrix} \Delta_{mn}^+ & -iA\eta_{mn} \\ iA\eta_{mn} & \Delta_{mn}^- \end{pmatrix} \chi_n - \sum_n k_x^2 \begin{pmatrix} D_+ & 0 \\ 0 & D_- \end{pmatrix} \delta_{mn} \chi_n + \sum_n k_x \begin{pmatrix} 0 & A \\ A & 0 \end{pmatrix} \delta_{mn} \chi_n = 0.$$

Or, more simply

$$\sum_n S_{mn} \chi_n - k_x^2 \sum_n X_{mn} \chi_n + k_x \sum_n T_{mn} \chi_n = 0. \quad (5.5)$$

Where

$$S_{mn} = \begin{pmatrix} \Delta_{mn}^+ & -iA\eta_{mn} \\ iA\eta_{mn} & \Delta_{mn}^- \end{pmatrix}, \quad X_{mn} = \begin{pmatrix} D_+ & 0 \\ 0 & D_- \end{pmatrix} \delta_{mn}, \quad T_{mn} = \begin{pmatrix} 0 & A \\ A & 0 \end{pmatrix} \delta_{mn} \quad (5.6)$$

The equation (5.5) can be in a better form if we set up

$$S = \begin{pmatrix} S_{11} & S_{12} & \dots & S_{1N} \\ S_{21} & S_{22} & \dots & S_{2N} \\ \cdot & \cdot & \dots & \cdot \\ \cdot & \cdot & \dots & \cdot \\ \cdot & \cdot & \dots & \cdot \\ S_{N1} & S_{N2} & \dots & S_{NN} \end{pmatrix}, X = \begin{pmatrix} X_{11} & X_{12} & \dots & X_{1N} \\ X_{21} & X_{22} & \dots & X_{2N} \\ \cdot & \cdot & \dots & \cdot \\ \cdot & \cdot & \dots & \cdot \\ \cdot & \cdot & \dots & \cdot \\ X_{N1} & X_{N2} & \dots & X_{NN} \end{pmatrix} \quad (5.7)$$

$$T = \begin{pmatrix} T_{11} & T_{12} & \dots & T_{1N} \\ T_{21} & T_{22} & \dots & T_{2N} \\ \cdot & \cdot & \dots & \cdot \\ \cdot & \cdot & \dots & \cdot \\ \cdot & \cdot & \dots & \cdot \\ T_{N1} & T_{N2} & \dots & T_{NN} \end{pmatrix}, K = \begin{pmatrix} \chi_1 \\ \chi_2 \\ \cdot \\ \cdot \\ \cdot \\ \chi_N \end{pmatrix}.$$

Noting that  $S_{mn}, X_{mn}, T_{mn}$  are  $2 \times 2$  matrices and is  $2 \times 1$  matrix, so  $S, X, T$  are  $2N \times 2N$  matrices and  $K$  is the  $2N \times 1$  matrix. After this setting we have (5.5) in the form

$$S\kappa - k_x^2 X\kappa + k_x T\kappa = 0. \quad (5.8)$$

We can get to the form of Eigen problem with  $k_x$  is eigenvalues if we do as follow

$$F = k_x \kappa \quad (5.9)$$

and then (5.8) becomes

$$S\kappa + TF = k_x XF. \quad (5.10)$$

If we consider E.q (5.9) and E.q (5.10) as equations of  $K$  and  $F$  variables, we can rewrite E.q (5.9) and E.q (5.10) in the form of the matrix equation

$$\begin{pmatrix} 0 & 1 \\ S & T \end{pmatrix} \begin{pmatrix} \kappa \\ F \end{pmatrix} = \begin{pmatrix} k_x & 0 \\ 0 & k_x X \end{pmatrix} \begin{pmatrix} \kappa \\ F \end{pmatrix}.$$

Let take  $k_x$  out of the matrix and move the matrix  $[1, 0; 0, X]$  into the left hand side by using its inverted matrix. We have

$$\begin{pmatrix} 1 & 0 \\ 0 & X \end{pmatrix}^{-1} \begin{pmatrix} 0 & 1 \\ S & T \end{pmatrix} \begin{pmatrix} \kappa \\ F \end{pmatrix} = k_x \begin{pmatrix} \kappa \\ F \end{pmatrix}. \quad (5.11)$$

Clearly the E.q (5.11) is the form of Eigen problem. So, for a given Energy we always completely determine  $k_x$  and  $K$  by E.q (5.11).

## 5.2 The wave function in each region and the equation to determine the coefficients $r_m, t_m$ .

For a given incident energy, we do not get one solution for  $k_x$ . The square matrix in E.q (5.11) has  $4N \times 4N$  dimensions, therefore the E.q (5.11) gives us  $4N$  solutions for  $k_x$  (example, if  $N=200$ , that means we have 800 solutions of  $k_x$ !). Because we have many eigen solutions, so we need to combine them in a superposition to get the correct wave function in each region. One thing makes us must do work carefully is the number of solutions. Number of solution of  $k_x$  is big, so we need to classify well to see that which wave is right-moving wave, which is left-moving wave. We will have both real solutions (propagated mode) and complex solutions (decay mode) for  $k_x$ .

For real momentum solutions, we can classify by calculating group velocities. If the group velocity is positive that means the wave is moving along the positive direction. It is a right-moving wave. Otherwise, the group velocity is negative, we have a left-moving

wave.

To calculate group velocities for real momentum solutions, we use the velocity operator which we can get from the Hamiltonian

$$\hat{v}_x = \frac{1}{\hbar} \frac{\partial H}{\partial k_x} = \frac{1}{\hbar} \left[ -2k_x \begin{pmatrix} D_+ & 0 \\ 0 & D_- \end{pmatrix} + \begin{pmatrix} 0 & A \\ A & 0 \end{pmatrix} \right] = \frac{1}{\hbar} [-2k_x X_0 + T_0] \quad (5.12)$$

Where

$$X_0 = \begin{pmatrix} D_+ & 0 \\ 0 & D_- \end{pmatrix}, \quad T_0 = \begin{pmatrix} 0 & A \\ A & 0 \end{pmatrix}. \quad (5.13)$$

The propagated direction is x direction. Group velocity along the x direction will be integrated over y from 0 to W. And we have

$$\begin{aligned} v_x &= \int_0^W dy \cdot \psi^\dagger \hat{v}_x \psi \\ &= \int_0^W dy \cdot e^{-ik_x x} \sum_n (\chi_n)^\dagger \cdot \varphi_n(y) \frac{1}{\hbar} [2i \cdot X_0 \cdot \partial_x + T_0] e^{ik_x x} \sum_m \chi_m \cdot \varphi_m(y) \\ &= \frac{1}{\hbar} \sum_n (\chi_n)^\dagger [-2k_x \cdot X_0 + T_0] \chi_n. \end{aligned} \quad (5.14)$$

For complex solutions of  $k_x$ , we can not classify by the group velocity. We will classify by the property of wave function at infinite. We know that the wave function should be 0 at infinite. So if a complex  $k_x$  in the form (general form of a complex number  $k_x = a + ib$ , the wave will in the form  $exp(i.kx.x) = exp[i(a+ib)x] = exp(iax) * exp(-bx)$ . For right-moving waves, the wave must be 0 at  $x = +\infty$ , so it requires  $b > 0$ . And for left-moving waves, the wave function must be 0 at  $x = -\infty$ , so it requires  $b < 0$ . Before we write wave functions in each region, we will make a nice form for eigenstate (5.1). We combined all in a unique form of K vector. So, we can do similar thing for sine function  $\varphi_n(y) = \sqrt{\frac{2}{W}} \sin(\frac{n\pi y}{W})$ . We also combine all sine functions in a vector, a row vector as  $\varphi(y) = \begin{pmatrix} \varphi_1(y) & \varphi_2(y) & \dots & \varphi_N(y) \end{pmatrix}$  is a row matrix N elements. Then (5.1) can be

written as

$$\psi(x, y) = e^{ik_x x} \cdot \varphi(y) \kappa. \quad (5.15)$$

Now we can write wave functions for the left, middle, right regions. Each region has wave function as following:

$$\begin{aligned} \psi^L(x, y) &= e^{i.k_n^L.x} \cdot \varphi(y) \kappa_{n,I}^L + \sum_{m=1}^{2N} r_m \cdot e^{i.k_m^L.x} \cdot \varphi(y) \kappa_m^{L,-} \\ \psi^M(x, y) &= \sum_{m=1}^{2N} a_m \cdot e^{i.k_m^M.x} \cdot \varphi(y) \kappa_m^{M,+} + \sum_{m=1}^{2N} b_m \cdot e^{i.k_m^M.x} \cdot \varphi(y) \kappa_m^{M,-} \\ \psi^R(x, y) &= \sum_{m=1}^{2N} t_m \cdot e^{i.k_m^R.x} \cdot \varphi(y) \kappa_m^{R,+}. \end{aligned} \quad (5.16)$$

The plus (+) notation indicates for the waves which are right-moving waves, and the minus (-) notation indicates for left-moving waves. The coefficients  $r_m, a_m, b_m, t_m$  will be solved by the continuity conditions. We have two continuity conditions for wave functions: the wave functions and their first derivative are continuous at the two interfaces  $x = 0$  and  $x = \ell$ :

$$\begin{cases} \psi^L(x=0, y) = \psi^M(x=0, y) \\ \partial_x \psi^L(x=0, y) = \partial_x \psi^M(x=0, y) \end{cases} \quad \& \quad \begin{cases} \psi^M(x=\ell, y) = \psi^R(x=\ell, y) \\ \partial_x \psi^M(x=\ell, y) = \partial_x \psi^R(x=\ell, y) \end{cases} \quad (5.17)$$

These 4 equations lead to the following equations after some calculations

$$\begin{cases} \kappa_{n,I}^L = - \sum_{m=1}^{2N} r_m \cdot \kappa_m^{L,-} + \sum_{m=1}^{2N} a_m \cdot \kappa_m^{M,+} + \sum_{m=1}^{2N} b_m \cdot \kappa_m^{M,-} \\ k_{n,x,I}^L \cdot \kappa_{n,I}^L = - \sum_{m=1}^{2N} r_m \cdot k_{m,x}^L \cdot \kappa_m^{L,-} + \sum_{m=1}^{2N} a_m \cdot k_{m,x}^M \cdot \kappa_m^{M,+} + \sum_{m=1}^{2N} b_m \cdot k_{m,x}^M \cdot \kappa_m^{M,-} \\ 0 = \sum_{m=1}^{2N} a_m \cdot e^{i.k_m^M.x} \cdot \ell \cdot \kappa_m^{M,+} + \sum_{m=1}^{2N} b_m \cdot e^{i.k_m^M.x} \cdot \ell \cdot \kappa_m^{M,-} - \sum_{m=1}^{2N} t_m \cdot e^{i.k_m^R.x} \cdot \ell \cdot \kappa_m^{R,+} \\ 0 = \sum_{m=1}^{2N} a_m \cdot k_{m,x}^M \cdot e^{i.k_m^M.x} \cdot \ell \cdot \kappa_m^{M,+} + \sum_{m=1}^{2N} b_m \cdot k_{m,x}^M \cdot e^{i.k_m^M.x} \cdot \ell \cdot \kappa_m^{M,-} - \sum_{m=1}^{2N} t_m \cdot k_{m,x}^R \cdot e^{i.k_m^R.x} \cdot \ell \cdot \kappa_m^{R,+} \end{cases}$$

If we set up

$$r = \begin{pmatrix} r_1 \\ r_2 \\ \cdot \\ \cdot \\ \cdot \\ r_{2N} \end{pmatrix}, a = \begin{pmatrix} a_1 \\ a_2 \\ \cdot \\ \cdot \\ \cdot \\ a_{2N} \end{pmatrix}, b = \begin{pmatrix} b_1 \\ b_2 \\ \cdot \\ \cdot \\ \cdot \\ b_{2N} \end{pmatrix}, t = \begin{pmatrix} t_1 \\ t_2 \\ \cdot \\ \cdot \\ \cdot \\ t_{2N} \end{pmatrix}$$

$$\begin{aligned} \kappa^{L,-} &= [\kappa_1^{L,-}, \kappa_2^{L,-}, \dots, \kappa_{4N}^{L,-}], \kappa^{M,+} = [\kappa_1^{M,+}, \kappa_2^{M,+}, \dots, \kappa_{4N}^{M,+}], \kappa^{M,-} = [\kappa_1^{M,-}, \kappa_2^{M,-}, \dots, \kappa_{4N}^{M,-}] \\ G_{n,I}^L &= k_{n,x,I}^L \cdot \kappa_{n,I}^L \\ G_m^{L,-} &= k_{m,x}^{L,-} \cdot \kappa_m^{L,-} \rightarrow G^{L,-} = [G_1^{L,-}, G_2^{L,-}, \dots, G_{4N}^{L,-}] \\ G_m^{M,+} &= k_{m,x}^{M,+} \cdot \kappa_m^{M,+} \rightarrow G^{M,+} = [G_1^{M,+}, G_2^{M,+}, \dots, G_{4N}^{M,+}] \\ G_m^{M,-} &= k_{m,x}^{M,-} \cdot \kappa_m^{M,-} \rightarrow G^{M,-} = [G_1^{M,-}, G_2^{M,-}, \dots, G_{4N}^{M,-}] \\ P_m^{M,+} &= e^{i.k_{m,x}^{M,+} \cdot \ell} \cdot \kappa_m^{M,+} \rightarrow P^{M,+} = [P_1^{M,+}, P_2^{M,+}, \dots, P_{4N}^{M,+}] \\ P_m^{M,-} &= e^{i.k_{m,x}^{M,-} \cdot \ell} \cdot \kappa_m^{M,-} \rightarrow P^{M,-} = [P_1^{M,-}, P_2^{M,-}, \dots, P_{4N}^{M,-}] \\ P_m^{R,+} &= e^{i.k_{m,x}^{R,+} \cdot \ell} \cdot \kappa_m^{R,+} \rightarrow P^{R,+} = [P_1^{R,+}, P_2^{R,+}, \dots, P_{4N}^{R,+}] \\ Q_m^{M,+} &= k_{m,x}^{M,+} e^{i.k_{m,x}^{M,+} \cdot \ell} \cdot \kappa_m^{M,+} \rightarrow Q^{M,+} = [Q_1^{M,+}, Q_2^{M,+}, \dots, Q_{4N}^{M,+}] \\ Q_m^{M,-} &= k_{m,x}^{M,-} e^{i.k_{m,x}^{M,-} \cdot \ell} \cdot \kappa_m^{M,-} \rightarrow Q^{M,-} = [Q_1^{M,-}, Q_2^{M,-}, \dots, Q_{4N}^{M,-}] \\ Q_m^{R,+} &= k_{m,x}^{R,+} e^{i.k_{m,x}^{R,+} \cdot \ell} \cdot \kappa_m^{R,+} \rightarrow Q^{R,+} = [Q_1^{R,+}, Q_2^{R,+}, \dots, Q_{4N}^{R,+}]. \end{aligned} \tag{5.18}$$

We can rewrite the equations in the form of matrix equation:

$$\begin{pmatrix} \kappa_{n,I}^L \\ G_{n,I}^L \\ 0 \\ 0 \end{pmatrix} = \begin{pmatrix} -\kappa^{L,-} & \kappa^{M,+} & \kappa^{M,-} & 0 \\ -G^{L,-} & G^{M,+} & G^{M,-} & 0 \\ 0 & P^{M,+} & P^{M,-} & -P^{R,+} \\ 0 & Q^{M,+} & Q^{M,-} & -Q^{R,+} \end{pmatrix} \begin{pmatrix} r \\ a \\ b \\ t \end{pmatrix}. \tag{5.19}$$

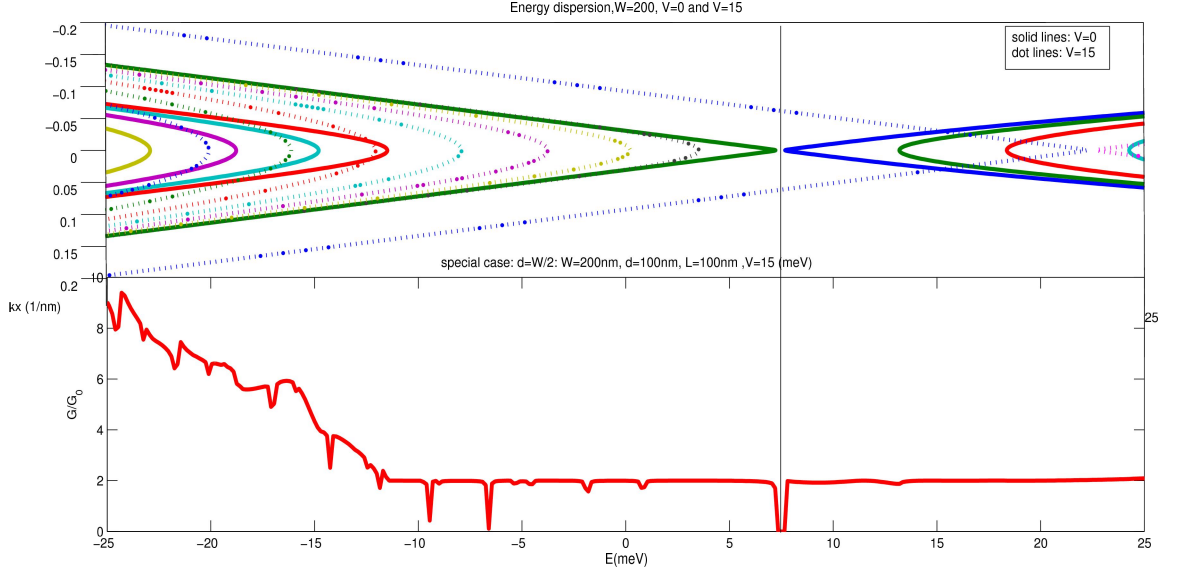


Figure 5.2: Conductance of the system for the special case  $d=W/2$ . Other parameters are  $W=200\text{nm}$ ,  $\ell=100$ ,  $V=15\text{meV}$ .

### 5.3 Results of conductance and discussion.

The conductance of the system can be computed by the formula

$$G = G_0 \sum_{n=1}^{N_{k_x^{L,+} \text{real}}} T_n = G_0 \sum_{n=1}^{N_{k_x^{L,+} \text{real}}} \sum_{m=1}^{N_{k_x^{R,+} \text{real}}} |t_{m;n}|^2 \cdot \frac{v_m^{R,+}}{v_n^{L,+}}. \quad (5.20)$$

Here  $G_0 = \frac{e^2}{h}$ . With (5.14) helps us to calculate group velocities and (5.19) helps us to compute  $t_{m;n}$  for each incident wave. Thus we have completely factors to determine conductance by (5.20).

In the Fig. 5.2 we show the conductance of the quantum transport system is versus incident energy in the case of  $d = W/2$ . For this case, our result is identical to the Kai Chang group's in the reference [5] And in the Fig. 5.3 we show the conductance of the quantum point contact system versus energy, the width of potential areas is  $d=20\text{nm}$ , the width of the system is  $W=200\text{nm}$ . Look at both figures we can see that the conductance spectra have sharp transmission dips. However, in the quantum point contact system some sharp transmission dips are removed when incident energy line is just crossing the



CHAPTER 5. QUANTUM TRANSPORT IN HGTE/CDTE QUANTUM POINT CONTACT.

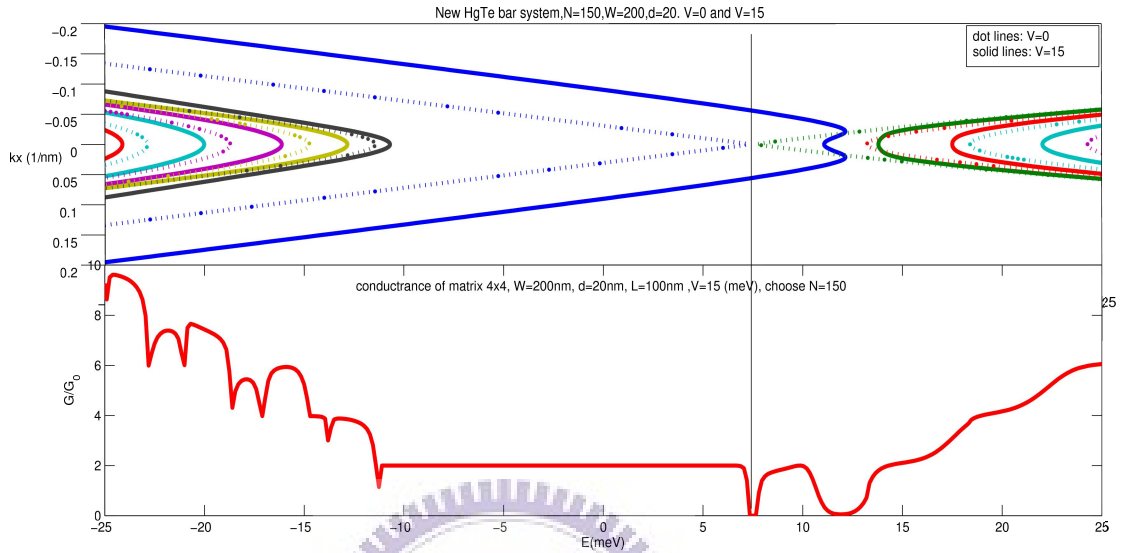


Figure 5.3: Conductance of the system.  $W=200\text{nm}$ ,  $d=20\text{nm}$ ,  $\ell =100\text{nm}$ ,  $V=15\text{meV}$ .

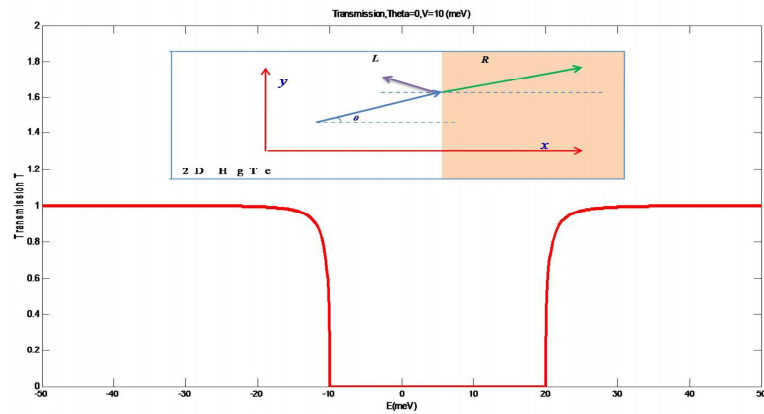


Figure 5.4: Transmission in 2D HgTe/CdTe system with 1 interface,  $V=10\text{meV}$ . No resonance states.

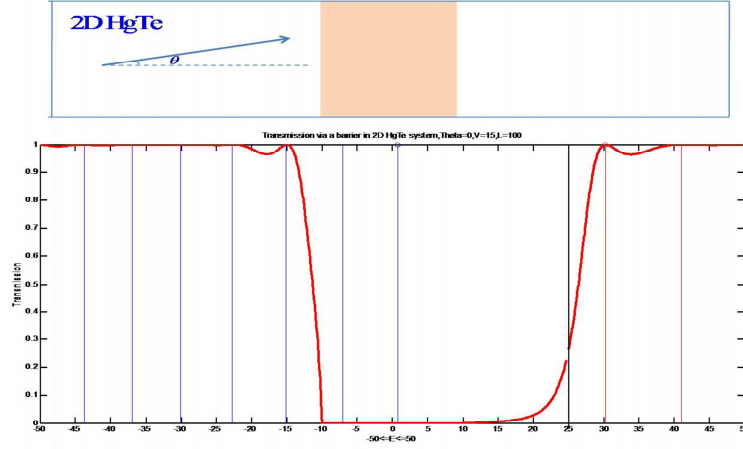


Figure 5.5: Transmission in 2D HgTe/CdTe system with 2 interfaces,  $V=10\text{meV}$ ,  $\ell=100\text{nm}$ . Some broad resonance states appear.

edge states. To understand the appearance of the sharp transmission dips, let start from the results in the 2D HgTe/CdTe systems. The Fig. 5.4 shows us the transmission in the 2D HgTe/CdTe system with 1 interface. In this system we have 2 regions with different potentials and we have no boundaries. The transmission result does show any peak. Meanwhile, the system 2D HgTe/CdTe with 2 interfaces has some resonance peaks in the transmission spectrum. But these peaks are broad resonances. They are not sharp transmission dips as the spectra in the Fig. 5.2, 5.3. So we can understand that the sharp transmission dips in the spectra Figs. 5.2 and 5.3 are sharp resonances and they appear because of boundary condition of the system. This also means that edge states are reason of the appearance of the sharp resonances. Normally the resonance states can be understood in the following interpretation [14], [15]: For the highest peaks with transmission is perfect, the energies which are corresponding to these peaks can be found from discrete energy levels of the box corresponds to the middle region. To find the energy levels of the box, we just need to replace  $k_x = n.\pi/L$  and insert into the equation which allows us to determine energy dispersion. A similar work is carried out for the 2D HgTe/CdTe system with 2 interfaces and we can see energy lines in the Fig. 5.5 which are indicated for the energy levels of the corresponding box. In the Fig. 5.5 we can see

that, when incident energy hits one energy level of the box, the transmission reaches to the perfect transmission. For the lowest peaks, we can explain by using leaking modes for the middle region. In the spectra Figs. 5.2 and 5.3 the interpretation is based on the resonance of edge states and some other states. However, we do still not know exactly at which energy that sharp resonances appear. So, this for this dark point we would like propose as a discussion that we are expecting to know the answer.



# Chapter 6

## Conclusion and proposal for future work.

### 6.1 Conclusion

Throughout the thesis, we have shown that HgTe/CdTe is a 2D topological insulator material via calculating Berry curvature, Chern number and  $Z_2$  invariant of this material. Besides, by the works in chapter 3 we showed for HgTe/CdTe quantum Hall bar system, there are 2 pairs of edge states appear at boundaries. The couple edge states in the influence of time reversal symmetry locate at the same boundary, moving in opposite directions, and have the opposite spin directions. While the couple edge states with the same spin direction, locate at different boundaries and moving in opposite directions. The second method in chapter 3 showed a nice analytical result of edge states for the semi-infinite system.

In chapter 4 we proposed a new system which is just applied potentials at transverse boundaries, we call it is the two split gates system. In this system we show that edge states still locate at boundaries even something changed. The results also show that the shifts of sub bands are different under effect of the potentials. Specifically, edge states are affected much more than bulk states. Under the influence of the potentials of the electric

gates, the edge gap can be opened bigger or closer. Besides, if the potentials are strong enough, they can destroy edge states around the gamma point.

In chapter 5, we have studied quantum transport in the HgTe/CdTe quantum point contact we see that in the conductance spectra, some sharp resonance dips appear due to the interference between edge states and evanescent states. In this part, we can explain the appearance of the sharp resonances. For the interpretation that exactly which energy that sharp resonances appear, we would like to propose as a discussion.

## 6.2 Future work.

In this work we can see that edge states are still located at near edges in the two split gates system. So, from the result we would like to propose a new project is finding the way to destroy these edge states. If we can do that, that means we can control transmission of edge states in a topological material. This is very interesting. Because edge states are general features of topological insulators, they are protected by time reversal symmetry. Hence if we want to destroy edge states, we can find a way to break down time reversal symmetry. A good way is using magnetic field. When we apply magnetic field, we need to calculate again Hamiltonian of 3D model, this work we should start from 8x8 Kane model. And then calculate effective Hamiltonian of model which we are interested in before we consider behavior of edge states under effect of magnetic field. It is a big work, so this idea we would like to propose it as a future work.

# Appendix A

## Appendix

We have  $\varphi_n(y) = \sqrt{\frac{2}{W}} \sin\left(\frac{n\pi y}{W}\right)$

Substituting into the formula of  $\eta_{mn}$ , then

$$\begin{aligned}\eta_{mn} &= \langle \varphi_m(y) | k_y | \varphi_n(y) \rangle = \int_0^W dy \cdot \sqrt{\frac{2}{W}} \sin\left(\frac{m\pi y}{W}\right) (-i \frac{\partial}{\partial y}) \sqrt{\frac{2}{W}} \sin\left(\frac{n\pi y}{W}\right) \\ &= -i \frac{2m\pi}{W^2} \int_0^W dy \cdot \frac{1}{2} \left[ \sin\left(\frac{m+n}{W}\pi y\right) + \sin\left(\frac{m-n}{W}\pi y\right) \right] \\ &= i \frac{n\pi}{W^2} \left[ \frac{W}{(m+n)\pi} \cos\left(\frac{m+n}{W}\pi y\right) + \frac{W}{(m-n)\pi} \cos\left(\frac{m-n}{W}\pi y\right) \right] \Big|_0^W \\ &= i \frac{n\pi}{W^2} \left[ \frac{W}{(m+n)\pi} \cos[(m+n)\pi] - \frac{W}{(m+n)\pi} + \frac{W}{(m-n)\pi} \cos[(m-n)\pi] - \frac{W}{(m-n)\pi} \right] \\ &= i \frac{n\pi}{W^2} \frac{2mW}{(m^2-n^2)\pi} [(-1)^{m+n} - 1].\end{aligned}$$

This result is just correct for  $m \neq n$ . For  $m=n$ , we have

$$\begin{aligned}\eta_{mm} &= \langle \varphi_m(y) | k_y | \varphi_m(y) \rangle = \int_0^W dy \cdot \sqrt{\frac{2}{W}} \sin\left(\frac{m\pi y}{W}\right) (-i \frac{\partial}{\partial y}) \sqrt{\frac{2}{W}} \sin\left(\frac{m\pi y}{W}\right) \\ &= -i \frac{2m\pi}{W^2} \int_0^W dy \cdot \sin\left(\frac{m\pi y}{W}\right) \cos\left(\frac{m\pi y}{W}\right) \\ &= \langle \varphi_m(y) | k_y | \varphi_m(y) \rangle \\ &= -i \frac{m\pi}{W^2} \int_0^W dy \cdot \sin\left(\frac{2m\pi y}{W}\right) \\ &= 0.\end{aligned}$$

To calculate  $\Delta_{mn}^+, \Delta_{mn}^-$  we need to start from  $\langle \varphi_m(y) | k_y^2 | \varphi_n(y) \rangle$ .

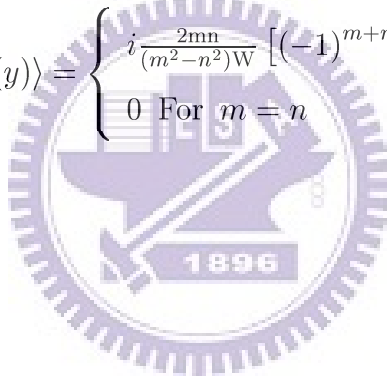
$$\begin{aligned} \langle \varphi_m(y) | k_y^2 | \varphi_n(y) \rangle &= \int_0^W dy \cdot \sqrt{\frac{2}{W}} \sin\left(\frac{m\pi y}{W}\right) \left(-i \frac{\partial}{\partial y}\right)^2 \sqrt{\frac{2}{W}} \sin\left(\frac{n\pi y}{W}\right) \\ &= \left(\frac{n\pi}{W}\right)^2 \frac{2}{W} \int_0^W dy \cdot \sin\left(\frac{m\pi y}{W}\right) \sin\left(\frac{n\pi y}{W}\right) = \left(\frac{n\pi}{W}\right)^2 \cdot \delta_{mn} \end{aligned}$$

Thus,

$$\Delta_{mn}^+ = (C + V + M) \delta_{mn} - D_+ \langle \varphi_m(y) | k_y^2 | \varphi_n(y) \rangle = (C + V + M) \delta_{mn} - D_+ \left(\frac{n\pi}{W}\right)^2 \cdot \delta_{mn}$$

$$\Delta_{mn}^- = (C + V - M) \delta_{mn} - D_- \langle \varphi_m(y) | k_y^2 | \varphi_n(y) \rangle = (C + V - M) \delta_{mn} - D_- \left(\frac{n\pi}{W}\right)^2 \cdot \delta_{mn}$$

$$\eta_{mn} = \langle \varphi_n(y) | k_y | \varphi_m(y) \rangle = \begin{cases} i \frac{2mn}{(m^2 - n^2)W} [(-1)^{m+n} - 1] & \text{For } m \neq n \\ 0 & \text{For } m = n \end{cases}$$



# Bibliography

- [1] Xiao-Liang Qi and Shou-Cheng Zhang, *physics today*, January 2010.
- [2] Hai-Zhou Lu, Wen-Yu Shan, Wang Yao and Shun-Qing Shen, *Phys. Rev. B* **81**, 115407 (2010).
- [3] Wen-Yu Shan, Hai-Zhou Lu and Shun-Qing Shen, *New Journal of Physics* **12** (2010) 043048.
- [4] Bin Zhou, Hai-Zhou Lu, Rui-Lin Chu and Qian Niu, *Phys. Rev. Lett.* **101**, 246807 (2008).
- [5] L. B. Zhang, Feng Zhai and Kai Chang, *Phys. Rev. B* **81**, 235323 (2010).
- [6] L. B. Zhang, F. Cheng, F. Zhai, and Kai Chang, *Phys. Rev. B* **83**, 081402(R) (2011).
- [7] Markus Knig, Steffen Wiedmann, *Science* **318**, 766 (2007).
- [8] C.L Kane, E. J. Mele, *Phys. Rev. Lett.* **95**, 146802 (2005).
- [9] B.A Bernevig, S-C.Zhang, *Phys. Rev. Lett.* **96**, 106802 (2006).
- [10] B.A Bernevig, T.L Hughes, S-C.Zhang, *science* **314**, 1757 (2006).
- [11] F.D.M Haldane, *Phys. Rev. B* **61**, 2015 (1988).
- [12] Berry, M. V, Proceedings of the Royal Society of London. A. *Mathematical and Physical Sciences* **392** (1802): 45-57.



## BIBLIOGRAPHY

---

- [13] Di Xiao, Qian Niu, *Rev. Of. Modern. Phys*, Volume **82**, July-September 2010.
- [14] A. Uma Maheswari, P. Prema, and C. S. Shastry, *Am. J. Phys.*, Vol. **78**, No. 4, 412 (2010).
- [15] Naomichi Hatano, Keita Sasada, *arXiv*: **0705.1388**.

